NASA TECHNICAL NOTE

NASA TN D-2720

NASA TN D-2720

INVESTIGATION OF DAMAGE TO BRITTLE MATERIALS BY IMPACT WITH HIGH-VELOCITY PROJECTILES INTO GLASS AND LUCITE

by James H. Diedrich and Francis S. Stepka

Lewis Research Center
Cleveland, Ohio

NATIONAL AERONAUTICS AND SPACE ADMINISTRATION • WASHINGTON, D. C. • MARCH 1965

NASA TN D-2720

INVESTIGATION OF DAMAGE TO BRITTLE MATERIALS BY IMPACT WITH HIGH-VELOCITY PROJECTILES INTO GLASS AND LUCITE

By James H. Diedrich and Francis S. Stepka

Lewis Research Center
Cleveland, Ohio

NATIONAL AERONAUTICS AND SPACE ADMINISTRATION

For sale by the Office of Technical Services, Department of Commerce,
Washington, D.C. 20230 -- Price $2.00

INVESTIGATION OF DAMAGE TO BRITTLE MATERIALS BY IMPACT WITH HIGH-VELOCITY PROJECTILES INTO GLASS AND LUCITE

by James H. Diedrich and Francis S. Stepka

Lewis Research Center

SUMMARY

An investigation was made to determine the effect of variables influencing the extent of damage incurred by brittle materials subjected to impact loading by high-velocity projectiles. The specimens investigated covered a wide range of sizes and geometric shapes, such as solid cylinders, circular disks, rectangular prisms, triangular prisms, tubes, and specimens with abrupt changes in cross section. The effect of holes or voids in the specimens was also investigated.

The specimens were divided into two general classifications: thin targets that were completely penetrated by the projectile and thick targets that were able to resist perforation. Glass and Lucite were employed as target materials to permit a rapid, visual qualitative examination of surface and subsurface damage details. The majority of the data were obtained by using 7/32-inch-diameter spherical aluminum projectiles traveling at about 6400 feet per second.

The results of the investigation indicated that the primary damage directly associated with the projectile penetration and crater damage are determined by the target and projectile material and the impact conditions. Secondary damage caused by the reflections and the interactions of the induced pressure waves was shown to be dependent upon the size and the shape of the target.

The results also indicated that the method of target support and the materials contacting the target boundaries can influence the extent of secondary damage. The use of appropriate backing materials was found to reduce the extent of secondary damage in thick targets that were not completely penetrated by the projectile. Thin targets, however, generally exhibited an increase in secondary damage when backing materials were employed.

INTRODUCTION

Analysis of space electric power systems (ref. 1) has indicated that the waste-heat radiator can comprise a substantial portion of the total powerplant weight. The majority of the radiator weight is concentrated in the protective armor on the radiator surfaces vulnerable to damage by impacting meteoroids. Analytical comparisons on the basis of total radiator weight (ref. 2) for a given level of protection nominate materials that are not ideal structurally. The materials producing the lowest value of weight for a radiator with high no-puncture probability operating in the temperature range from 1200° to 1400° F in a high-power system are beryllium, graphite, and molybdenum in order of increasing radiator weight. Other materials such as stainless steel and columbium alloys produce radiators having around five times the weight of a beryllium radiator for the configurations and protection criteria considered in reference 2. Beryllium and graphite radiators were also shown theoretically to be potentially lighter than aluminum radiators in the temperature range from 600° to 800° F.

There is great incentive then to use radiator armor materials such as beryllium, graphite, and molybdenum when striving for low values of powerplant specific weight. However, these materials were nominated primarily on the basis of their ability to resist penetration by impacting projectiles, secondary consideration being given to thermal conductivity, and density. Currently the impact resistance is taken as a function of an empirical cratering criterion which involves a strength property such as the modulus of elasticity (ref. 3). The true behavior of some of these materials of interest under high-velocity impact, however, is for the most part unknown.

In testing beryllium with high-velocity particles, cracking and spalling was found to occur in sheets and tubes in addition to the normal impact crater. Preliminary data (ref. 4) suggest that this may be a general characteristic of brittle materials under high-velocity impact. It was felt, therefore, that a separate qualitative study should be made of the causes of this cracking behavior in order to understand the phenomena, determine the influencing factors, and find the most effective and least complex means of reducing or preventing such damage. The study was initiated to determine qualitative effects of the suspected variables on the severity of cracking and spalling in typically brittle materials. These variables were target size, target shape, and other materials in contact with the target boundaries.

Glass and cast, transparent methyl methacrylate plastic (Lucite or Plexiglas) were chosen as the materials for the study because of their known brittle nature and for the fact that their transparency permits a rapid, visual qualitative examination of surface and subsurface damage details. The scope of the investigation was limited for most of the data to a projectile velocity of approximately 6400 feet per second with a 7/32-inch-diameter aluminum projectile accelerated with a 220-caliber Swift rifle. The impact

Mach number, or ratio of projectile velocity to the acoustic velocity in the target material, was 0.34 for glass targets and 0.72 for Lucite targets. At an impact Mach number of 0.72, the resulting damage in Lucite is similar to hypervelocity impact damage in beryllium in that the damage in the immediate vicinity of the point of impact has a similar appearance (ref. 5). The other external fractures are located correspondingly in both classes of materials; however, their intensity and extent are greater in the metals than in the Lucite. At the time of this writing an internal examination of the beryllium targets had not been performed; hence, the similarity of the damage cannot be extended beneath the external surface.

The glass and Lucite specimens investigated covered a wide range of geometric shapes and were divided into two general classifications: thin targets that were completely penetrated by the projectile and thick targets that were able to resist complete penetration. Target size, target shape, and various materials in contact with the specimen boundaries were investigated to assess their relative significance on the observed damage. The principal criterion used in the analysis of impact damage is a qualitative visual examination of the location and severity of the cracking damage.

SYMBOLS

C_L longitudinal velocity

C_t transverse velocity

E modulus of elasticity

G shear modulus

ρ density

σ_i incident stress wave

σ_r reflected stress wave

σ_t transmitted stress wave

ν Poisson's ratio

APPARATUS

Projectile Accelerator

A 220-caliber Swift high-speed rifle was used to accelerate the projectiles. The

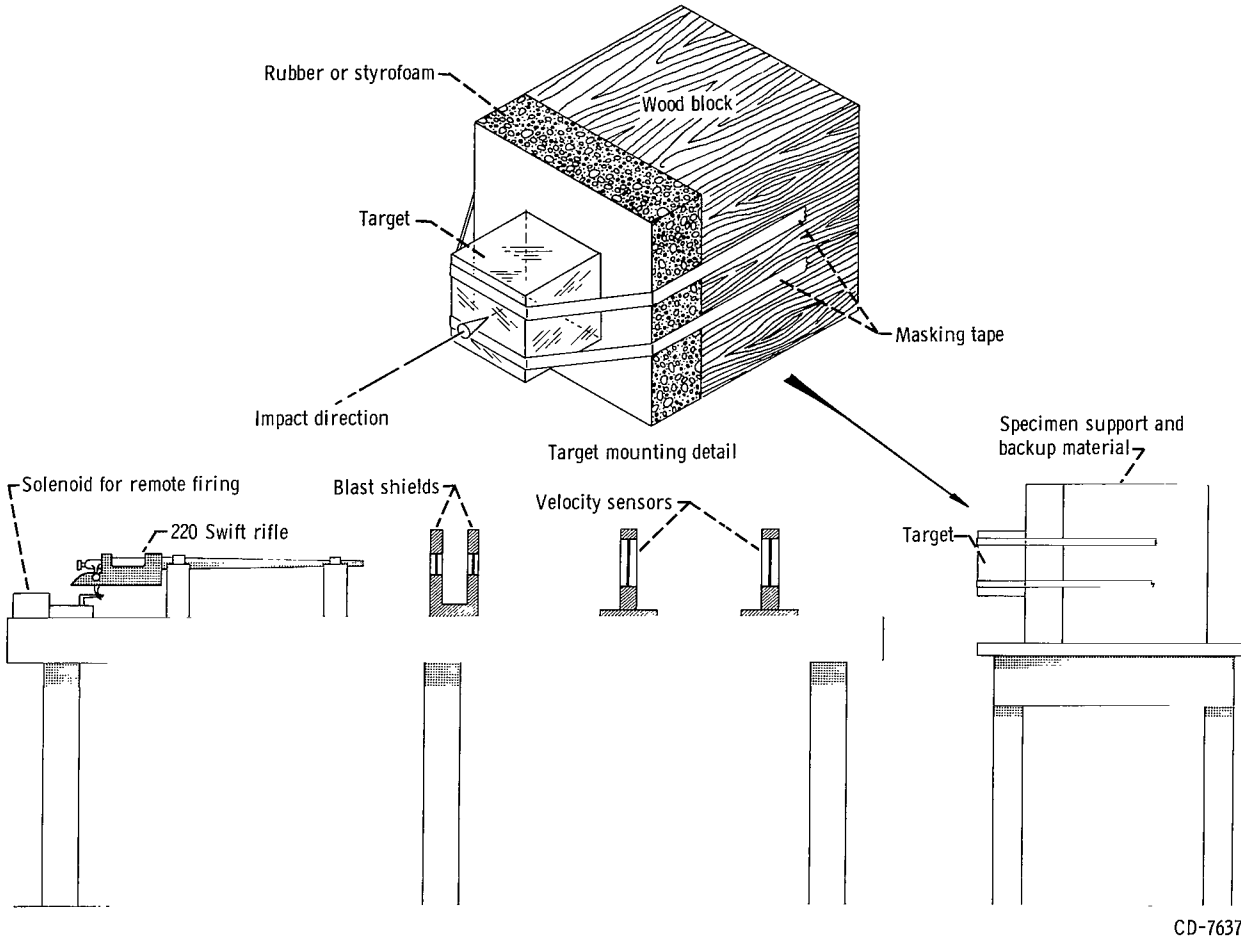

Figure 1. - Projectile accelerator.

rifle was mounted on a table and fired remotely (fig. 1). The powder charges were varied to control the velocity of the projectiles. The projectiles were mostly 7/32-inch-diameter spheres of aluminum, and they impacted the specimens at a nominal velocity of 6400 feet per second. Besides the aluminum projectiles, specimens were impacted with 7/32-inch-diameter spheres of nylon, glass, and steel, and the velocities of these projectiles ranged from 2000 to 7500 feet per second.

Instrumentation

Projectile velocity measurement. - A pair of sensors to measure the projectile velocity were located 1 foot apart, 2 feet, and 3 feet, respectively, downstream of the gun barrel (fig. 1). Each sensor consisted of a 1/4-mil Mylar sheet with a layer of vapor-deposited aluminum approximately 100 angstroms thick on each side of the Mylar. Perforation of each of the sensors by a projectile resulted in the shorting of the two

layers of aluminum of the sensor, which permitted a capacitor to discharge. The successive discharge pulses were monitored by an electric event timer. The maximum error in velocity measurement was estimated to be 1.0 percent and was caused primarily by the dimensional variations in the location of the sensors.

High-speed framing camera. - In order to permit observation of the pressure waves generated by impact and the reflection of the waves from the free surfaces of the targets, a shadowgraph of the progress of the waves was obtained by the use of a continuous-writing high-speed framing camera. The camera writing rate used was about 250 000 frames per second. The illumination for the shadowgraph was supplied by backlighting the transparent specimens with a xenon lamp. Perforation of a sensor similar to that used for projectile velocity measurement provided a signal for the initiation of the light source.

Targets

The brittle target materials used in this investigation were plate glass and Lucite. The glass targets or specimens were square plates that ranged in size from 4 to 16 inches on each side or disks ranging from 4 to 16 inches in diameter. The thickness of the specimen was either 1/8 or 1/4 inch. Steel-wire reinforced glass was also investigated. The Lucite targets were primarily 4- by 4- by 1-inch sheets or cylinders or tubes with an outside diameter of 2 inches and a length of 4 inches. Other shapes such as rectangular or triangular prisms were also investigated. The more complex Lucite shapes were annealed for 12 hours at 175° F to remove the stresses induced by machining. The effect on Lucite targets using backing material or laminations was investigated with materials such as rubber, wood, lead, paraffin, steel, and aluminum.

The impact face of the glass targets was covered with masking tape before impact to contain the glass for examination. The glass targets were either unsupported or were held with masking tape against a 1/4-inch-thick rubber sheet backed with a wood block to stop the projectile. The Lucite targets were either unsupported or were held with masking tape against a 10-inch block of styrofoam backed with a wood block to stop the projectile (fig. 1).

RESULTS AND DISCUSSION

The following section presents the observed results and an assessment of the individual effects of target size, shape, internal boundaries, internal reinforcement, and materials contacting the external boundaries. Prior to embarking on the presentation

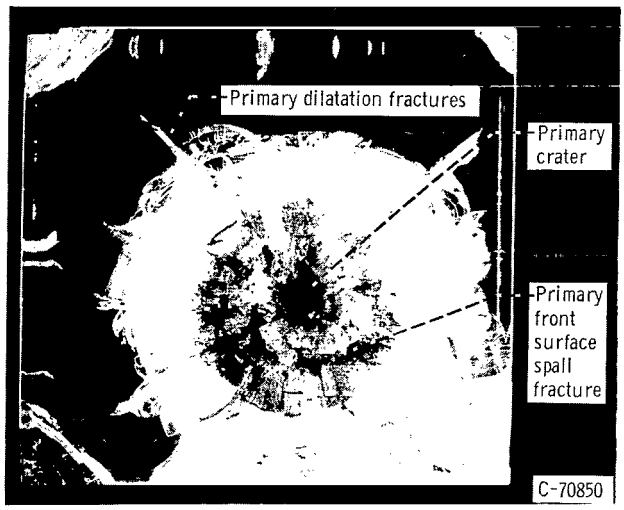

(a) Impact face.

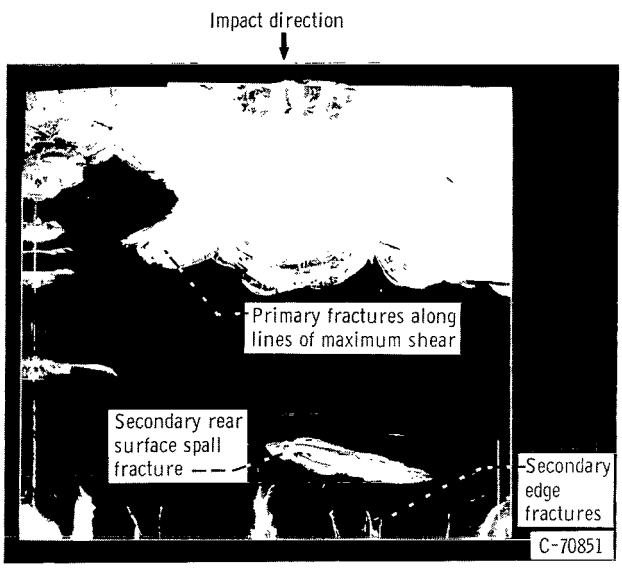

(b) Side view.

Figure 2. - Typical primary and secondary impact fractures in Lucite. Target, 4-inch cube; projectile, 7/32-inch-diameter aluminum sphere; velocity, 14 700 feet per second (ref. 5).

of the experimental results, some discussion is warranted on the general behavior of a brittle target when impacted by a high-velocity projectile. The ensuing discussion will be mainly a qualitative description of the phenomena and a description of the damage resulting from impact.

Damage Phenomena

Primary impact fractures. - The ensuing discussion will be based on typical impact fractures in a Lucite block obtained from reference 5 and illustrated in figure 2. The block was impacted with a 7/32-inch-diameter aluminum sphere at a velocity of 14 700 feet per second.

When a homogeneous, isotropic material is subjected to a localized impact by a particle, the material is locally crushed, and the particle penetrates into the material. The crushed material is ejected from the face of the target, and the impact crater is generated. The intense local pressure at the point of impact causes the specimen material to fail locally along a logarithmic spiral of maximum shear (ref. 6) and produces a front spall that results in the cup-shape depression surrounding the impact point in figure 2. The front spall has been found to be a discrete piece of material with a central hole. The fact that it was a discrete piece with a finite thickness confirms that the fracture severing it from the specimen started beneath the surface of the material, as shown in figure 2.

After the local crushing and plastic deformation has run its course, an elastic stress wave detaches from the crater area and propagates hemispherically through the specimen (ref. 7). In reality, two waves are produced in the specimen, a longitudinal and a transverse wave (ref. 8). These propagate through the specimen with distinct

velocities dependent on the elastic constants and the density of the medium. The longitudinal wave has associated particle motion parallel to the direction of propagation, and the strain is pure dilatation. The transverse wave has particle motion normal to the direction of propagation, and the strain is in the nature of shear. The expression for the velocity of the longitudinal wave (ref. 8) is

$$C_L = \left(\frac{\lambda + 2G}{\rho}\right)^{1/2} \tag{1}$$

where

$$\lambda = \frac{\nu E}{(1 + \nu)(1 - 2\nu)}$$

The expression for the transverse wave is

$$C_t = \left(\frac{G}{\rho}\right)^{1/2} = \left[\frac{E}{2\rho(1 + \nu)}\right]^{1/2} \tag{2}$$

The longitudinal wave propagates through the material with approximately twice the velocity of the transverse wave and is the major cause of fracture in the medium (ref. 8, p. 87). For the sake of brevity, the balance of the discussion will consider only the effects of the longitudinal wave.

Figure 3 indicates that the wave AB must expand to A'B' as the distance dr is traversed in an interval of time. The strain associated with the longitudinal wave promotes dilatation. If the load application is sudden, the material may not be able to sustain the rate of extension, and radial cracks or fractures will develop. The critical velocity of straining and the rate of energy application producing these radial fractures are related to the impact velocity. Their number will increase as the loading rate and the rate of energy application increase (ref. 8). These radial fractures have been observed in beryllium, molybdenum, glass, and Lucite specimens. It is anticipated that the shape of the specimen will also influence the number of such cracks.

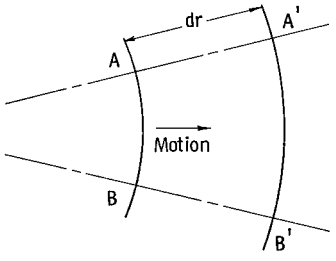

Figure 3. - Wavefront expansion.

As has been discussed, the impact produces three primary fracture phenomena in the specimen:

(1) Penetration and crushing

(2) Front spalling due to induced upward movement of the free surface and failure along trajectories of maxi-

mum shear

(3) Radial fractures due to dilatation of the material

These fractures are dependent solely on the properties of the material, on the energy and velocity of impact, and, in the case of item (3), on the shape and size of the specimen. There is little that can be done to reduce their severity for a given material and impact condition. In addition, these are the only type of fractures present in an infinite, homogeneous, isotropic medium.

Secondary impact fractures. - The stress waves propagate through the material until they are completely attenuated or until they react with a free surface or a different medium. A longitudinal stress wave at normal incidence upon a free surface is reflected as a longitudinal wave. A transverse wave at normal incidence upon a free surface is reflected as a transverse wave. At oblique incidence the results are much more complex since longitudinal and transverse waves can each reflect longitudinal and transverse components (ref. 8). The discussion will again consider only the primary longitudinal wave components, since the slower traveling transverse waves would not greatly influence the fracturing process.

When the free surface is replaced by a different medium, part of the incident longitudinal stress wave will be reflected, and part will be transmitted into the second medium as indicated in figure 4. The subdivision of the incident stress wave is dependent upon the properties of the two materials in contact.

The transmitted stress wave σ_t as a function of the incident stress wave σ_i is given by (ref. 9)

$$\sigma_t = \left(\frac{2}{1 + \frac{\rho_1 C_{L,1}}{\rho_2 C_{L,2}}} \right) \sigma_i \tag{3}$$

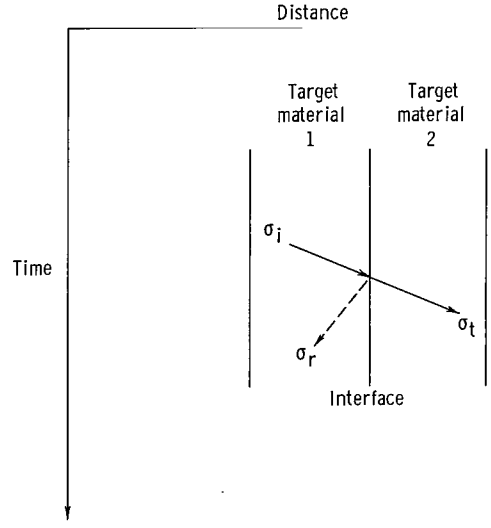

Figure 4. - Stress-wave transmission and reflection characteristics.

and the reflected stress wave is

$$\sigma_r = \left(\frac{1 - \frac{\rho_1 C_{L,1}}{\rho_2 C_{L,2}}}{1 + \frac{\rho_1 C_{L,1}}{\rho_2 C_{L,2}}} \right) \sigma_i \tag{4}$$

The product ρC_L is called acoustic impedance.

It is seen that, if the acoustic impedance of material 2 (the backing material) is very much larger than that of material 1, the re-

flected component is less than the incident stress wave and has the same sign as the incident stress wave (compression). If $\rho_2 C_{L,2} << \rho_1 C_{L,1}$, the reflected component approaches the value of the incident stress wave and is opposite in sign or tension. In the case of a free surface the reflected component is tensile and is equal to the value of the incident stress wave. Table I presents pertinent data for several materials of interest. Room-temperature data are shown unless otherwise noted. All data were obtained from references 9 to 12.

TABLE I. - ACOUSTIC PROPERTIES OF SELECTED MATERIALS

Material	Density, ρ, slugs/cu ft	Longitudinal velocity, C_L, ft/sec	Acoustic impedance, ρC_L, slugs/(sq ft)(sec)
Air	0.002378	1 170	2.7
Aluminum	5.22	20 900	109 000
Beryllium	3.59	41 400	148 600
Copper	17.2	14 900	257 000
Glass	5.22	19 000	99 000
Granite	5.23	10 400	54 300
Graphite	3.36	8 000	26 900
Lead	21.9	7 100	155 500
Lucite	2.32	8 700	20 200
Mercury	26.3	4 760	125 000
Molybdenum	19.8	18 300	363 000
Paraffin	1.74	4 160	7 250
Rubber	3.9	3 400	13 300
Steel	15.2	19 500	297 000
Vacuum	0	0	0
Water	1.94	4 860 (20° C)	9 430

Interactions between the reflected components of the incident stress waves can cause additional or secondary fractures apart from the primary impact fractures. These fractures occur when the local critical normal fracture stress of the material is exceeded (a dynamic property of the material, ref. 8, p. 29). The fractures appear in three distinct ways:

(1) Spalling - caused by the interaction between a reflected tension wave and a portion of the incident wave. Single or multiple spalls can occur.

(2) Dilatation - similar to the radial cracks produced by the expanding longitudinal stress waves in the impact area. These fractures are again radial in appearance and are caused by an expanding reflected tension disturbance. These fractures become apparent in brittle materials, particularly those weak in tension, and start at an interface and progress radially inward, toward the impact point.

(3) Internal fracture - caused by the reinforcement and interaction between the reflected components of the incident stress waves.

The behavior of these reflected waves and consequently the resulting fractures are greatly influenced by the acoustic impedance of the second medium or backing material. The second medium can be air, a vacuum, a liquid, or a solid. The shape of the specimen will also influence the location and the presence of the fracture described in item (3).

The reflection and transmission of an incident stress wave at an interface of two dissimilar materials also causes a time delay in the introduction of the components of the reflected waves in the brittle material. Their magnitude and time of appearance are principally regulated by the acoustic impedance and the thickness of the layers.

In summary, reflected components can cause secondary fractures in the specimen. These fractures are greatly influenced by the shape and size of the specimen and the acoustic impedance and thickness of the backing material and are therefore controllable.

Glass Plates

Size effects. - The influence of size of a glass-sheet target subjected to an impact by a high-velocity projectile is shown in figure 5(a). Shown is the result of impact into 1/8-inch-thick glass targets which were 4- by 4-, 8- by 8-, and 16- by 16-inch squares. It can be seen in figure 5(a) that extensive damage occurred to the smallest target, and less damage was encountered as the target size increased. Increasing the specimen size increases the amount of specimen material available to absorb the energy of impact. Consequently, the reflected pressure waves at the edge of the specimen are less intense for the larger specimen and are less likely to produce secondary cracking damage.

Shape effect. - The effect of target shape on the damage from the reflected pressure waves can be seen by comparing figure 5(b) with figure 5(a). Figure 5(b) illustrates that more damage is encountered across the smaller dimension of the 8- by 16-inch rectangle than across the larger dimension. The reason for this effect is that the incident pressure wave is more intense at the boundary formed by the narrow dimension. The more extensive fracturing at the corners of the rectangular and square specimens is the result of the meeting and reinforcement of the reflected waves.

To illustrate the effect of target shape on the secondary damage resulting from the reflected waves, impact was made into 16-inch-diameter sheets of glass. The results shown in figure 5(b) illustrate that less damage is sustained by a circular target than by rectangular and square targets of the same maximum dimension (figs. 5(a) and (b)). For a circular sheet target only a longitudinal wave is reflected from the free surface concentric with the impact point. Rectangular and square sheet targets exhibit a more complex set of circumstances since the longitudinal wave contacts the free target surface at oblique incidence and produces two reflected components. The interaction between the incident wave and the reflected components produces fractures along the target edges. The inset shown in figure 5(b) is an enlarged view of the primary crater damage and is typical of those encountered on all specimens in this series of experiments.

Effect of target boundary. - The results obtained with the glass targets already dis-

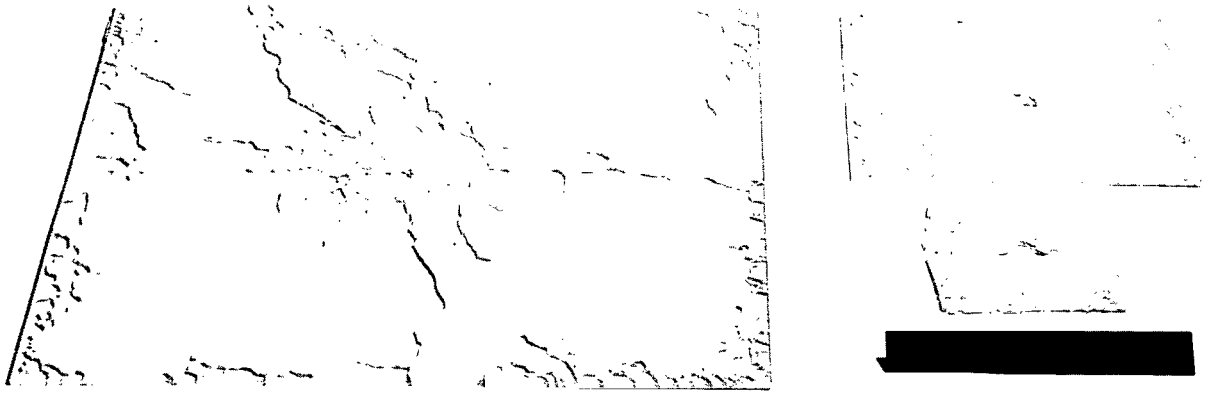

C-63887

(a) 4-, 8-, and 16-inch squares, 1/8-inch thick.

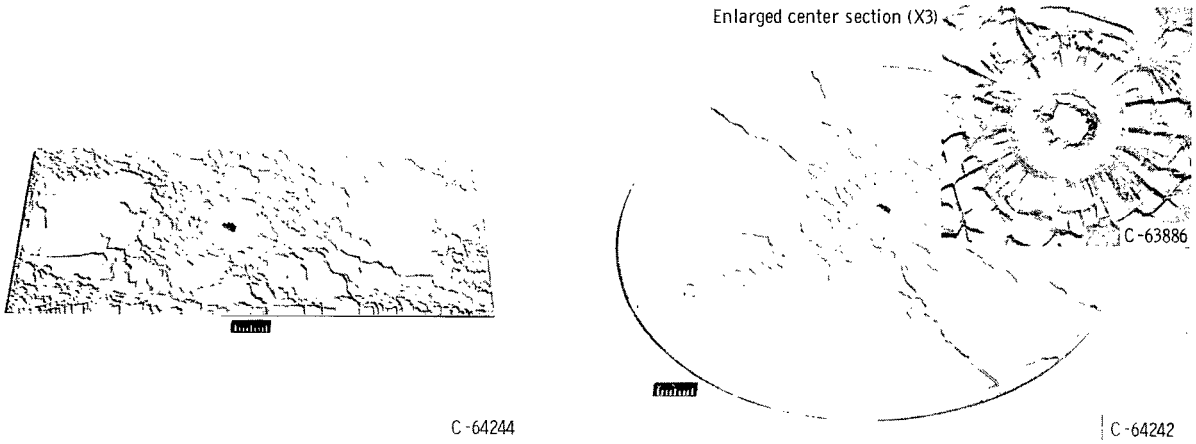

8 by 16 by 1/8 inch

16 inch diam by 1/8 inch

(b) Rectangular and circular sheet.

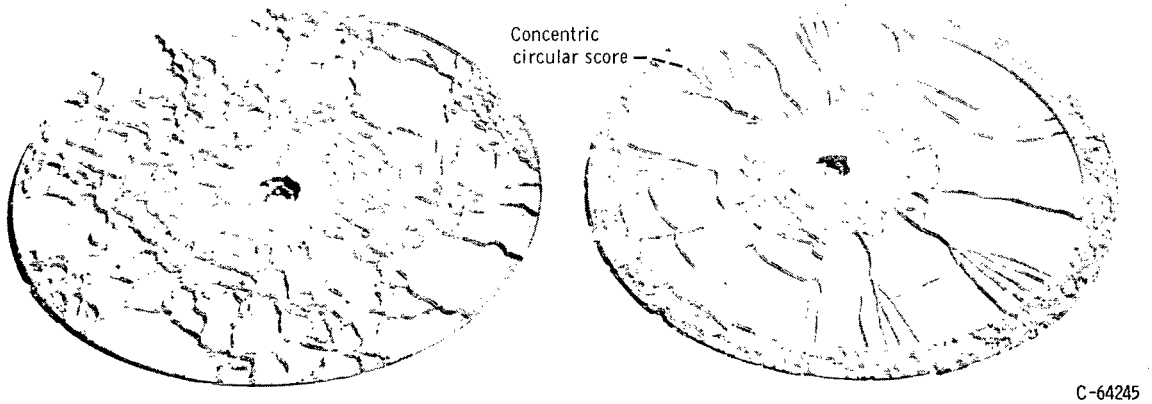

(c) Plain and scored 8-inch-diameter circular disks, 1/8-inch thick.

Figure 5. - Results of impact into glass sheets. Projectiles, 7/32-inch-diameter aluminum spheres; nominal velocity, 6400 feet per second.

cussed indicate that the damage in the vicinity of the penetration is a function of impact conditions and material, provided that the target size is large enough to eliminate the damaging effect of the tension waves reflected from target boundaries. These results suggest that damage control or reduction of damage in selected areas of the target can be accomplished by the control of the reflected waves from the target-free surfaces.

One method of reduction of damage in the vicinity of the impact in a small specimen would be to trap the energy of the reflected wave before it can return to the impact area. The effectiveness of this concept is illustrated in figure 5(c), which shows the result of an impact into two 8-inch-diameter glass plates. One of the plates had a concentric circular score, made by a glass cutter on one side about 1/2 inch from the outer edge. The depth of the score mark was limited to about 0.005 inch or about 4 percent of the thickness of the glass plate. What in effect occurs after impact is a spalling of the outer ring after the tension waves reached the section weakened by the score mark; thus a portion of the energy of the waves was trapped, and further reflections of the waves were kept within the outer ring. The result is extensive fracturing in the outer ring and less damage in the central region than in the unscored target. A deeper score mark would have interfered with the initial passage of the wave, and the outer ring would have been less effective in trapping the energy of the incident wave.

Other illustrations of the use of this concept are shown in figure 5(d), which shows the result of lightly scoring a 16- by 16-inch glass plate and the result of impact into a completely severed square of a 16- by 16-inch glass plate. The specimens were made by first covering one face of the glass plate with masking tape and then scoring the opposite face with a glass cutter. The first target was left in this condition, while the second specimen was cracked through along the score marks. The tape retained the individual square pieces of the target. It can be seen that the light scoring permitted the pressure wave to travel to the outer boundaries of the glass plate, but that on reflection most of the energy of the wave was trapped in the last score line around the outer edge of the target. The results of impact into the severed plate indicate that most of the energy of impact was reflected from the severed free boundaries and trapped in the central section. Some of the energy was transmitted across the interface, damaging the section directly beneath the central section.

A visual comparison with figure 5(a) indicates approximately the same degree of damage was sustained by the 4- by 4-inch plate as on the center section of the completely severed target just described. Severing of the target, then, effectively reduces the target size and serves to concentrate the bulk of the secondary cracking damage around the point of impact.

Effect of interior reinforcement. - Because glass and other brittle materials are relatively weak in tension, and since tension waves are responsible for a large part of the damage to targets impacted by high-speed particles, use of a material strong in ten-

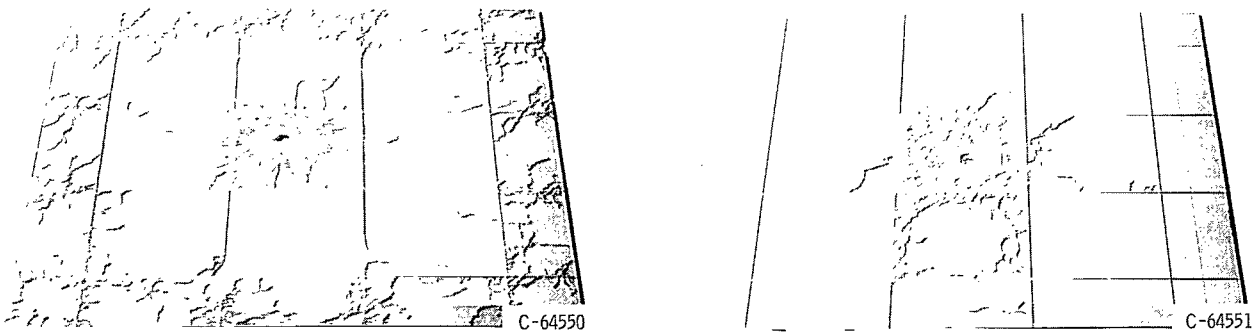

Lightly scored 4-inch squares

Severed 4-inch squares

(d) Scored 16-inch-square sheets, 1/8-inch thick.

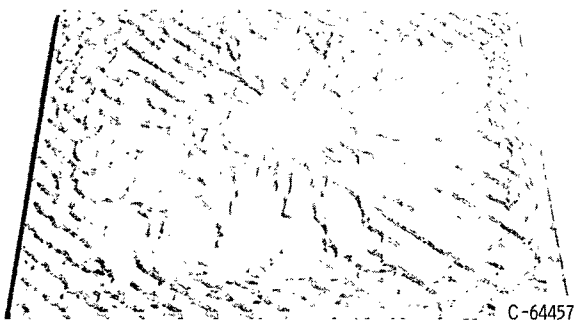

(e) Wire-reinforced 16-inch-square sheet, 1/4-inch thick.

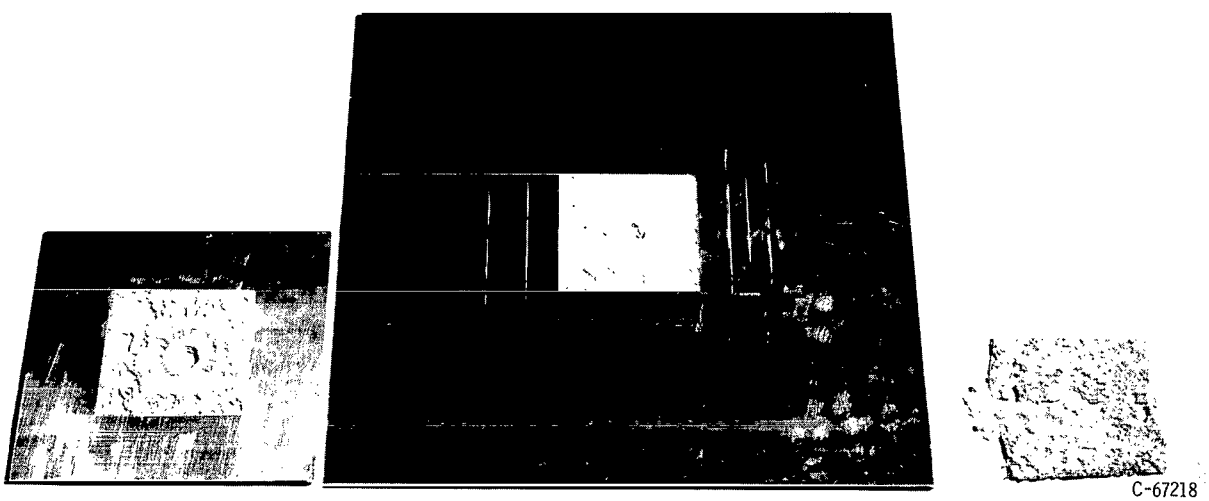

8-inch-square frame

16-inch-square frame

Plain specimen

(f) Comparison of aluminum-framed and plain 4-inch-square specimens, 18 inch thick.

Figure 5. - Concluded. Results of impact into glass sheets. Projectiles, 7/32-inch-diameter aluminum spheres; nominal velocity, 6400 feet per second.

sion to reinforce a matrix of brittle material may at first appear to be a method of reducing some of the damage. To investigate this concept, impacts were made into 1/4-inch-thick glass reinforced with steel wire. The plates were 16- by 16-inch squares having 0.020-inch-diameter wire reinforcements woven into mesh having approximately 1-inch openings. The results of impact of a typical specimen, shown in figure 5(e), indicate that the steel wire appears to provide a preferential locus for the fractures to occur. This damage is observed to be greater than that in the plain sheet of 16- by 16-inch square glass shown in figure 5(a).

Effect of adjacent materials. - It was expected that materials in contact with the target free boundaries would alter the reflection of the incident pressure waves. This characteristic was studied by surrounding glass plates of various sizes with a closely fitting frame of aluminum. The edges of the glass were first ground smooth and flat and hand fitted to an aluminum frame within 0.0005 inch. Aluminum was chosen as the frame material because its acoustic impedance (product of acoustic velocity and density) closely matched that of the glass. This means that an incident pressure wave arriving at a glass-aluminum interface would have the maximum transmission with the minimum reflection and thus result in less secondary cracking damage.

The specimens made were 4- by 4-inch glass inserted into 8- and 16-inch square aluminum frames. The damage around the crater was reduced somewhat by employing the aluminum frames. There was no apparent reduction in the observed damage to the glass specimen when frames of increasing size were employed, as shown in figure 5(f). However, the variation in contact area and contact force at the glass-aluminum interface caused some fracturing at the specimen edges and confused the damage pattern. It is indicated, however, that a degree of damage reduction in the specimen is possible by adjoining materials to the free boundaries. The areas immediately surrounding the impact points are quite similar to the same area on the 16- by 16-inch glass plate in figure 5(a) (p. 11). Elimination of the reflection of the pressure waves at the free boundaries close to the impact point or attenuating the magnitude of these reflected waves reduces the damage in the region of the crater.

The effectiveness of damage reduction by this method is strongly dependent on specimen size. The remarks made earlier on the effect of specimen size on the overall damage to the specimen (fig. 5(a)) should be recalled here.

Thick Lucite Sheet

The experiments performed on glass provided an insight into the cracking damage in thin sheets and indicated the desirability for obtaining further data by using thick plates and three-dimensional targets. For the initial study, thick sheet material which would

not be completely penetrated by the projectile was used. Glass was excluded from consideration as a material in this phase because of the difficulties encountered in its fabrication and its extreme sensitivity to crack propagation. A preliminary screening test indicated that a cast, transparent methylmethacrylate (i. e., Lucite or Plexiglas) exhibited the required brittle fracture behavior under impact and could readily be fashioned into complex shapes. Experiments were conducted with projectiles of nylon, steel, glass, and aluminum impacting 4- by 4- by 1-inch cast Lucite targets over a range of velocities. The resulting damage associated with the aluminum and glass spheres traveling at a velocity of about 6400 feet per second had similarities in appearance to the external damage encountered in beryllium targets, as explained previously. It was arbitrarily decided to use aluminum projectiles for the majority of the experimental work. Glass projectiles were employed for purposes of comparison in selected cases.

Backing materials with low acoustic impedance. - In view of the influence of the target boundary material on the resultant impact damage, as discussed in the section Damage Phenomena, it became desirable to investigate the effect of method of specimen support and/or the effect of a laminated target construction. The backing materials used in the investigation were rubber, wood, styrofoam, sponge plastic, concrete, and paraffin. The thickness of the backing materials was a minimum of $1\frac{1}{2}$ inches. Pertinent property data for these materials appear in table I. The styrofoam- and sponge-plastic materials were open-cell structure and hence have approximately the same properties as air. There is considerable variability in the density and longitudinal wave velocity for individual specimens of concrete and rocks. No direct property data were available for concrete but granite data were included for illustrative purposes. The specimens were held firmly against the rigid backing by strips of masking tape. The free-standing target was supported only on its lower edge and located approximately 18 inches in front of a cushion of sponge plastic which retained the target after impact. The backing materials were in full contact with each target.

Figure 6(a) illustrates the results typical of the impacts into 4- by 4- by 1-inch-thick cast Lucite specimens backed with low-acoustic-impedance materials. All of the targets were damaged about equally and are shown in figure 6(a). Each target exhibited a front spall under the impact point, a primary crater with several short radial fractures emanating from the impact point, and a secondary rear spall which remained attached to the target. The targets mounted on rubber, wood, and sponge plastic had an appearance similar to the target mounted on styrofoam and hence are not shown in figure 6(a).

The low-acoustic-impedance paraffin was used to simulate the effect of a liquid behind a thick wall and to note whether the spalling at the back of the target would have sufficient energy to generate pressures in the paraffin to cause bursting of the Lucite specimen similar to the catastrophic bursting of a wall of liquid-filled tanks reported in

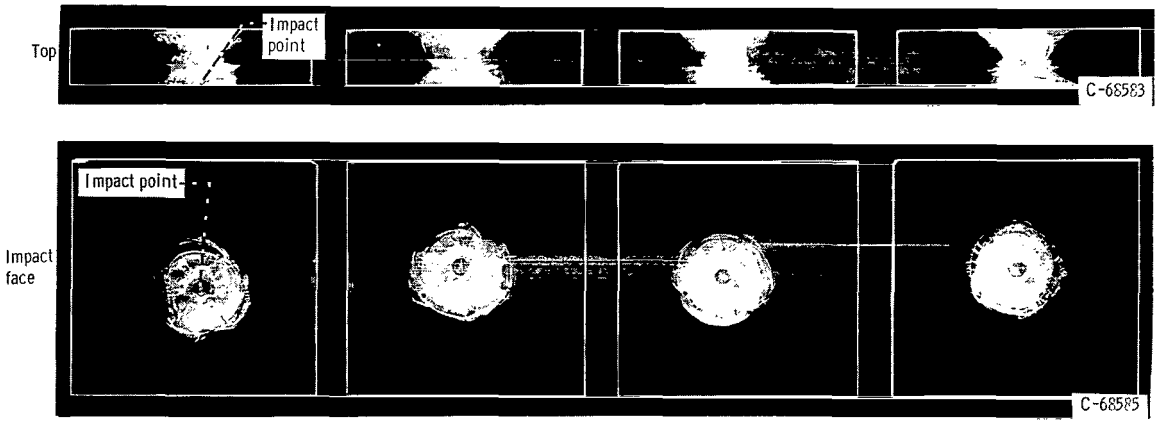

(a) Free-standing target and targets with low-acoustic-impedance backing materials (backing materials not shown).

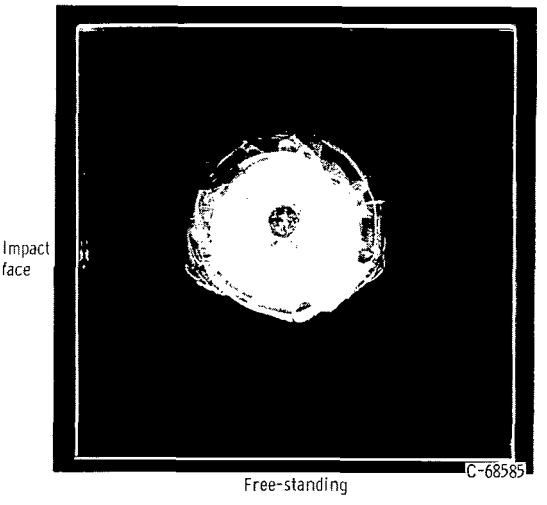

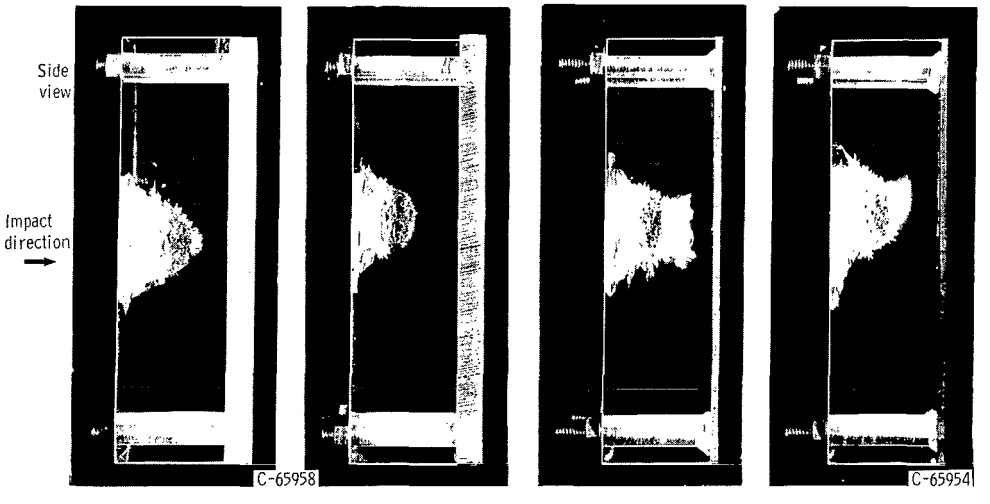

(b) Free-standing target and targets with high-acoustic-impedance backing materials.

Figure 6. - Results impact into 4- by 4- by 1-inch-thick nonperforated Lucite targets. Projectiles, 7/32-inch-diameter aluminum spheres; nominal velocity, 6400 feet per second.

reference 13. The thick targets, however, did not spall sufficiently to demonstrate catastrophic damage. The effects with thinner Lucite targets will be described in the section Thin Lucite Sheets.

Backing materials with high acoustic impedance. - Aluminum and lead were chosen to demonstrate the effect of high-acoustic-impedance backing materials. These materials have approximately the same acoustic impedances but represent opposite extremes in density. Two thicknesses of backing materials were tested: 1/16 and 1/4 inch. The results of impacts into these specimens are shown in figure 6(b). The expected similarity of damage between the 1/4-inch-thick lead and aluminum backed targets is clearly shown. As predicted in the previous section, there is a marked reduction in the amount of observed secondary damage when the high-acoustic-impedance backing is employed. In particular, the use of the backing sheets completely eliminated the back spall on the Lucite shown in the free-standing target in figure 6(a).

The experiments also illustrated the effect of thickness or mass of the backing material on the reappearance of reflected tensile-stress waves in the target. The 1/4-inch-thick plates resulted in a somewhat greater reduction in secondary damage than did the 1/16-inch-thick sheets for both lead and aluminum. These results appear to indicate that an arbitrary selection of target mounting material and thickness can produce questionable damage data unless the effects of the wave interaction in layered material are taken into account. For the scope of the present study, no consideration was given to optimizing the reduction in damage with the weights of the targets. It is felt that this should be done when specific structural materials or configurations of interest are investigated.

Thin Lucite Sheets

The results of the previous investigation on thick targets that were not completely penetrated by the projectile indicated that the acoustic impedance of the backing and its interaction with the Lucite target affected the character and extent of damage in the target. In each case the entire impact energy of the projectile was absorbed in the target. For thin targets that are completely penetrated by the projectile, the amount of impact energy absorbed by the target-backing combination is not constant. Thus, the damage to thin targets will not only be influenced by the acoustic impedance and by the interaction between the layered media but also by the amount of impact energy absorbed by the backing material and by any interaction from the energy absorption or resulting cratering process in the backing medium.

Free-standing targets. - For free-standing thin targets, where complete penetration occurs, only a portion of the energy of the impacting projectile is absorbed by the

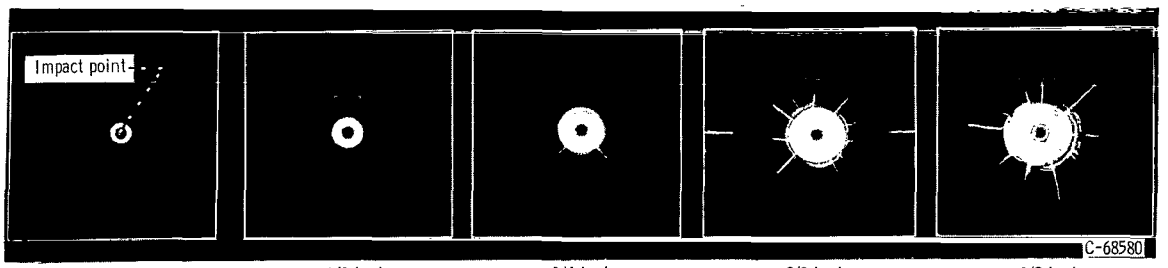

1/16 Inch 1/8 Inch 1/4 Inch 3/8 Inch 1/2 Inch

(a) Effect of specimen thickness on 4- by 4-inch free-standing targets.

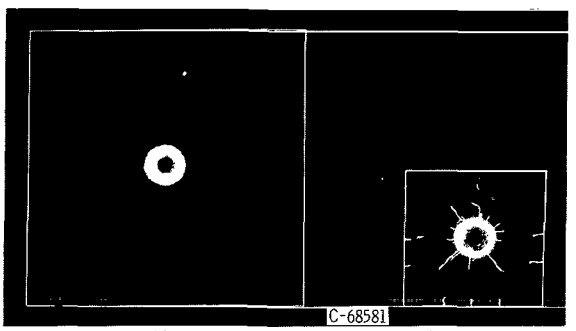

4 by 4 inches 2 by 2 inches

(b) Effect of target size on 1/8-inch-thick free-standing targets.

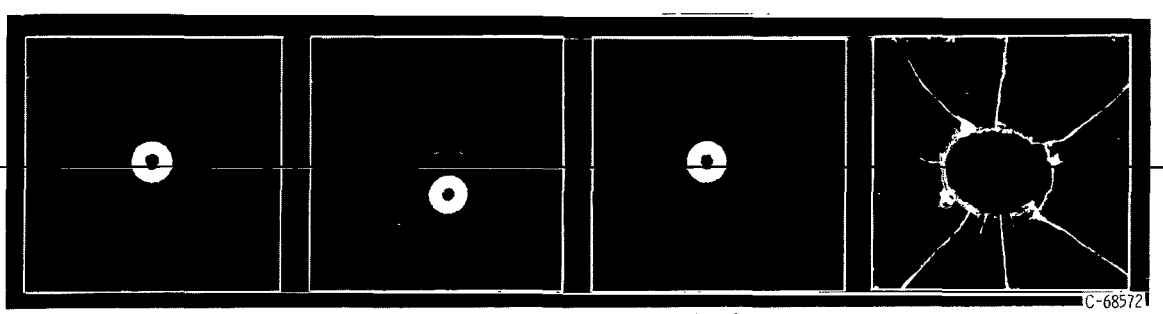

Free standing (no backing) Wood Styrofoam Paraffin

(c) Effect of low-acoustic-impedance backing materials on 4- by 4- by 1/2-inch-thick Lucite specimens (backing materials not shown).

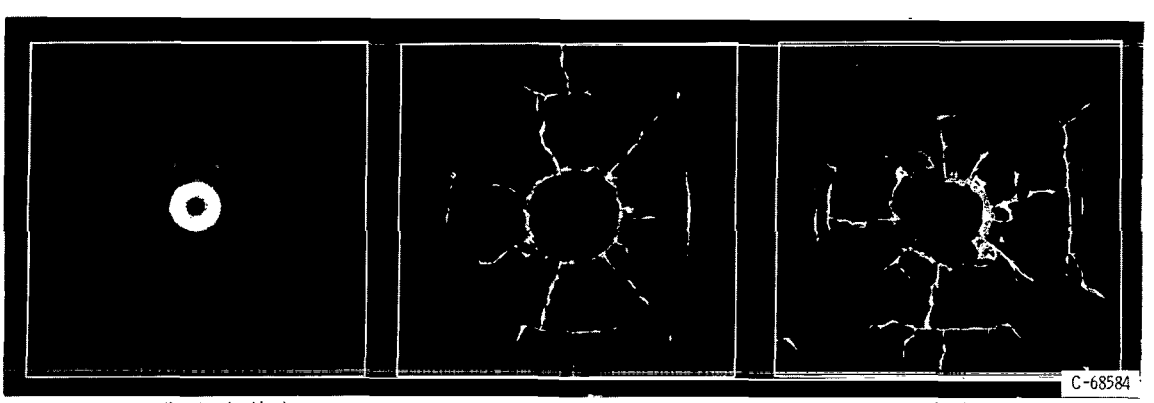

Free standing (no backing) Aluminum Lead

(d) Effect of high-acoustic-impedance backing materials on 4- by 4- by 1/8-inch-thick Lucite specimens (backing materials not shown).

Figure 7. - Results of impact into perforated Lucite targets. Projectiles, 7/32-inch-diameter aluminum spheres; nominal velocity, 6400 feet per second.

target. The amount of energy absorbed varies approximately with the square of the target thickness according to the results of reference 14. Consequently, as target thickness is decreased, a reduction in the observed damage would be expected for a given set of impact conditions. The results in figure 7(a) depict impact under the same conditions into free-standing 4- by 4-inch sheets of Lucite having thicknesses of 1/6, 1/8, 1/4, 3/8, and 1/2 inch. The results confirm the prior reasoning.

All of the targets tested had the same frontal dimensions, and therefore the results indicate only the effect of variation of thickness. Recalling the prior investigation using glass targets, changes in target size changed the induced damage. This observation was confirmed by using a 2- by 2- by 1/8-inch free-standing plastic target under the same conditions of impact as the 4- by 4- by 1/8-inch target (fig. 7(b)). The two targets had the same degree of damage immediately around the impact point; however, the smaller target suffered additional secondary damage from the stress waves reflected from the boundaries.

Backing materials with low acoustic impedance. - For these tests, impacts were made into 1/8-inch-thick, 4- by 4-inch targets of Lucite backed with wood, styrofoam, or paraffin. The thickness of the backing was approximately $1\frac{3}{4}$ inches. The results of the impacts shown in figure 7(c) indicate that the damage to the targets with wood and styrofoam was essentially the same as for the free-standing condition. The results of impact into the paraffin-backed target indicate considerably greater damage than with wood or styrofoam backing even though their acoustic impedances are approximately the same (table I). Liquid-filled tanks with thin metal walls exhibit a similar behavior when impacted by high-velocity projectiles (ref. 13). The causes of the observed catastrophic rupturing of the target with paraffin backing are conjectured to be the intense pressures generated in the paraffin in decelerating the projectile and the impact of the ejected paraffin backing material on the thin target. (Styrofoam and wood backing produced no observable ejecta under these particular impact conditions.) Increasing the target thickness, however, reduced the amount of impact energy absorbed in the target backing, which eliminated the induced rupture damage. Also, the thicker target was stronger and more able to resist the action of the ejected backing material and the pressure pulse. For Lucite target thicknesses of 3/8 inch and above, the resulting damage was similar to that in the free-standing counterparts.

Backing materials with high acoustic impedance. - Impacts were made into 1/8-inch-thick targets of Lucite, backed with $1\frac{1}{2}$-inch-thick lead and aluminum. The projectile completely penetrated the Lucite and was stopped by the lead or aluminum. The results obtained (fig. 7(d)) indicated large increases in damage compared to that in a free-standing 1/8-inch-thick target. This was in contrast to the results obtained when thick nonperforated targets were backed with the same materials (fig. 6(b)). In addition to the damage in the vicinity of the crater, secondary fractures at the sides of the thin Lucite

sheets were also obtained, plus radial fractures leading from the point of impact. The increase in damage when a backing material was used adjacent to a completely penetrated target was as expected, because the backing transferred some of the energy of the projectile back to the thin target, which contributed to the increase in damage.

The selection of materials for use as backings for thin targets that are completely penetrated by an impacting projectile cannot be made on the basis of acoustic impedance alone. In such cases, it has been demonstrated that the backing material participates in the primary cratering process, and thus its behavior under impact must also be taken into account.

The backing material ejected rearward along the direction of impact will strike the thin target and enlarge the initial primary crater in the relatively weak target. In addition the pressure wave induced in the backing material will be transmitted across the backing-target interface and induce additional secondary damage effects in the thin target. The use of paraffin, aluminum, and lead backing shown in figures 7(c) and (d) are illustrative of such processes. The projectile also penetrated deeper into the paraffin backing (approx. $1\frac{3}{4}$ in.) than into the aluminum or lead backing (approx. 0.20 in.). This observation suggests the generation of a less intense pressure pulse in the paraffin.

The results of the use of wood and styrofoam backing shown in figure 7(c) produced no observable increases in damage to the thin target. Projectiles penetrating such backing materials push the material aside, and relatively little material is ejected toward the target. Wood and styrofoam offered the least resistance to projectile penetration of any of the materials involved in this phase of the test and hence produced pressure pulses of relatively low intensity.

All of the processes just mentioned are involved in varying degrees in the generation of primary and secondary damage in thin target - backing-material combinations. Consequently, no one single explanation for the resulting damage can be given, since variations in target thickness and backing material cause different processes to be dominant. The reduction of secondary damage in thin targets that are completely penetrated by the projectile cannot be simply attained. Any additional materials affixed to the target faces will participate in the primary cratering process and consequently generate a pattern of damage peculiar to the combination of materials and impact condition. Generally, for a given set of impact conditions, the least damage sustained by a thin, brittle target is exhibited by the free-standing target itself. The addition of backing materials will, in general, increase the damage to the thin target.

Another implication of the preceding discussion is that, in a model study of the impact resistance of a particular design, the actual combination of materials involved should be used in the test application. In addition, any material used as a witness plate to stop a projectile after it penetrates a thin target should be located sufficiently far from the target to preclude the interaction of the material ejected from the witness plate

with the target.

Three-Dimensional and Shape Effects in Lucite Targets

Thus far the investigation has been restricted to normal impact on flat surfaces. However, it is known that the shape and size of the specimen can influence the wave reflections and interactions and cause secondary damage in undesirable locations. Inasmuch as space structures requiring protective meteoroid armor can assume a variety of shapes and often contain passages or channels for coolants, several target cross sections pertinent to typical space structures were tested.

In this phase of the study, emphasis was placed on means of analysis for predicting the influence of specimen shape and size on the location and severity of secondary damage and on the experimental verification of the predictions. In order to predict the location of secondary fractures, an understanding must first be gained of the reflection of an incident stress wave at free surfaces of various contours or at the interface of two dissimilar media. Consideration must be given to the effects caused by the specimen size and possible interactions by the energy absorption processes in adjacent media. In the analysis to follow, consideration is limited to a point source energy release as represented by impact from a small spherical projectile. Conditions not considered and beyond the scope of this report are deep penetrations or craters produced by jets or projectiles having large length-to-diameter ratios. The shape of the pressure wave produced by these latter items would alter the type and extent of damage incurred.

Specimen shape. - The effect of specimen shape on target damage is related to the stress-wave formation and reflection in the target. Recalling the prior discussion on the penetration and stress wave generation in thick targets (refer to the section Thick Lucite Sheet), it has been shown that longitudinal and transverse stress waves are induced in the target material. Again, only the longitudinal waves are considered in the following discussion.

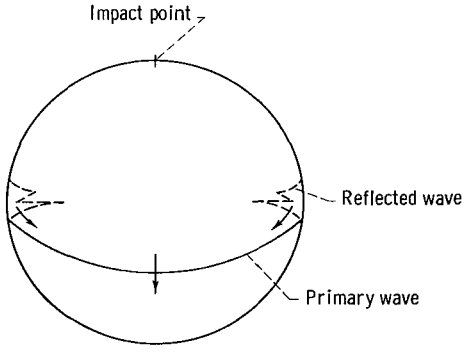

Figure 8. - Stress-wave reflection in cylindrical specimens.

Cylindrical specimens: The longitudinal wave reflection at the boundary of a solid circular cylinder produces reflected components that trail behind the primary wave front, as shown in figure 8 (ref. 8). As the wave progresses through the medium, the longitudinal waves reflected from the circular boundary are brought closer together until they interact. The anticipated fracture is located directly under the

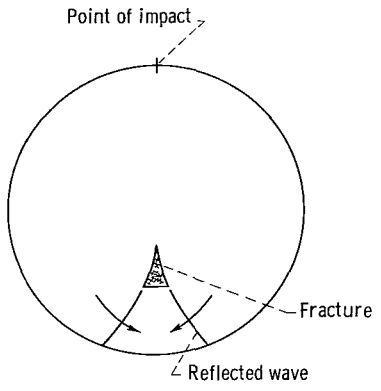

Figure 9. - Anticipated fracture in cylindrical specimens.

point of impact in the rear half of the specimen, as shown in figure 9, and is alined parallel to the direction of travel of the primary wave. Confirming observations of the progress of these waves were obtained from high-speed photographs of the impact into a plastic cylinder by observing the interference patterns of an intense light source through the transparent target. Also the location of the fracture was confirmed experimentally by using a solid Lucite model 2 inches in diameter and 4 inches long.

A second series of experiments was performed with tubular Lucite specimens 2 inches in diameter and 4 inches long, with a 1/2-inch-diameter hole bored along the central axis. The results are shown in figure 10. The fracture at the rear of the specimens, which was observed with both the aluminum and the glass projectiles, is the predicted secondary fracture. The fracture starts at the rear edge of the inner hole and propagates radially outward in the direction of impact. This result was observed in all subsequent tests. The presence of the central hole contributes to the location of the secondary damage fracture and apparently causes the reflected waves to interact with maximum effectiveness because of the lack of the supporting material removed by the hole.

Triangular prism specimens: Analysis of the effect of an impact into an apex of an equilateral triangular prism indicated that no secondary damage due to reflected waves should occur. No reflection of the incident primary wave occurs at the boundaries on either side of the impacted apex because the motion of the primary wave is parallel to the side boundaries. Reflection of the wave can only occur when the primary wave has moved across the specimen to the third side of the triangular prism opposite the impact point and normal to the primary wave. At this time secondary damage in the nature of a spall can occur when the wave is reflected if the energy of the wave is sufficiently high. The result of an impact into the apex of a solid triangular Lucite specimen, shown in figure 11, did not produce visible secondary damage.

Impact was also made normal to one of the prism faces to illustrate the effect of reflected waves from the side boundaries. It can be seen from the figure that, in addition to the crater, a fracture was formed at the center of the specimen as a result of the interaction of the tension waves produced from the reflections at the side boundaries. The result of an impact into the apex of a triangular prism with a central circular hole is also shown in figure 11. It can be seen that the presence of the hole provides a free surface for wave reflection and thus alters the results. Fractures were observed to occur at the edge of the hole extending toward the base of the crater.

Square prism specimens: In order to compare the damage in other shapes of specimens, impacts were made into a solid square prism and a square prism with a central

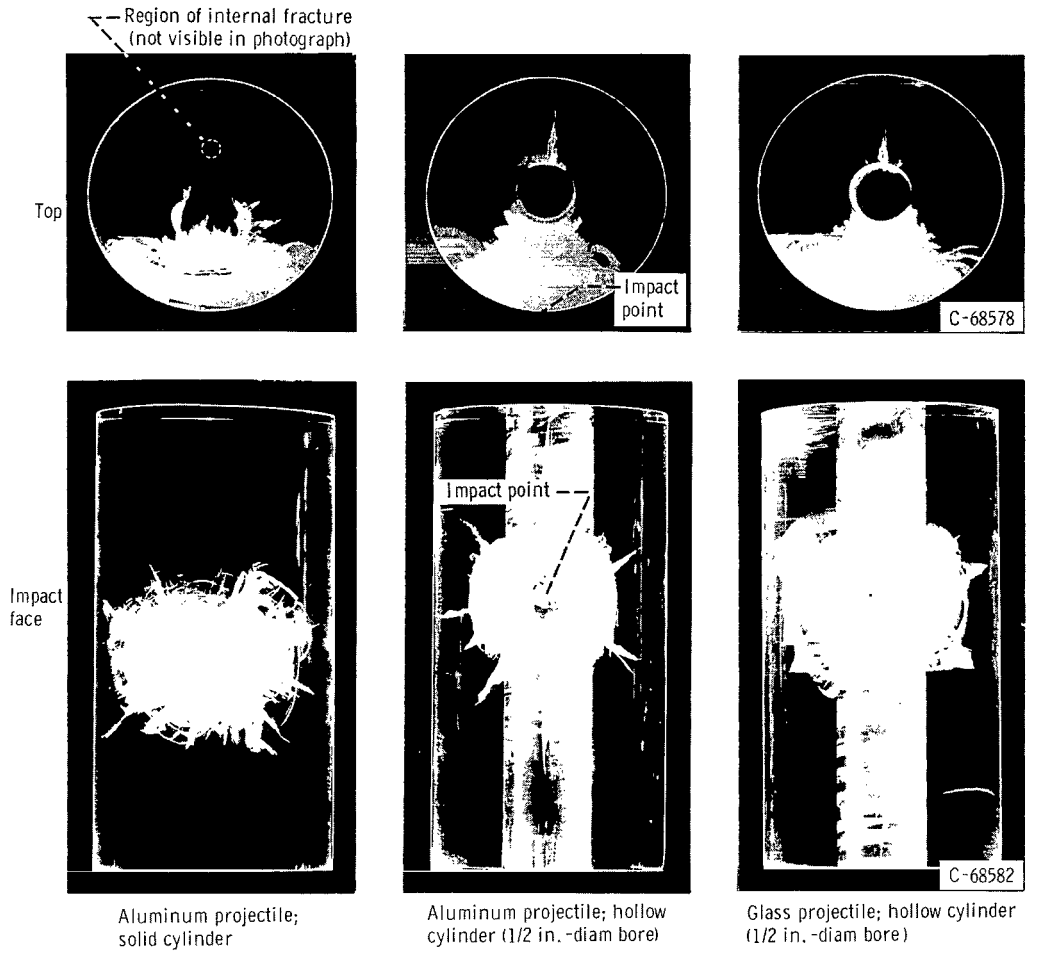

Figure 10. - Damage to Lucite cylinders (2-in. o.d., 4-in. length) resulting from impact by 7/32-inch-diameter spheres at nominal velocity of 6400 feet per second.

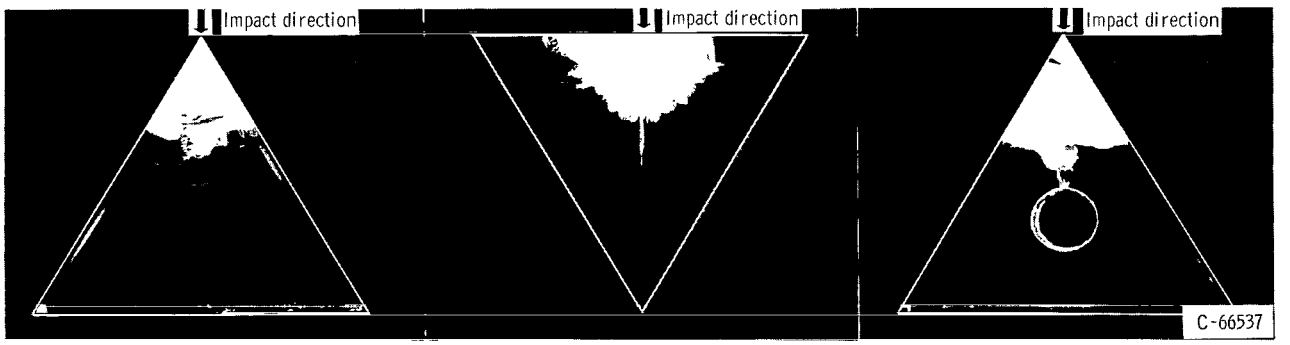

Figure 11. - Damage to triangular prisms ($2\frac{5}{8}$-in. sides, 4-in. length) resulting from impact by 7/32-inch-diameter aluminum spheres at nominal velocity of 6400 feet per second.

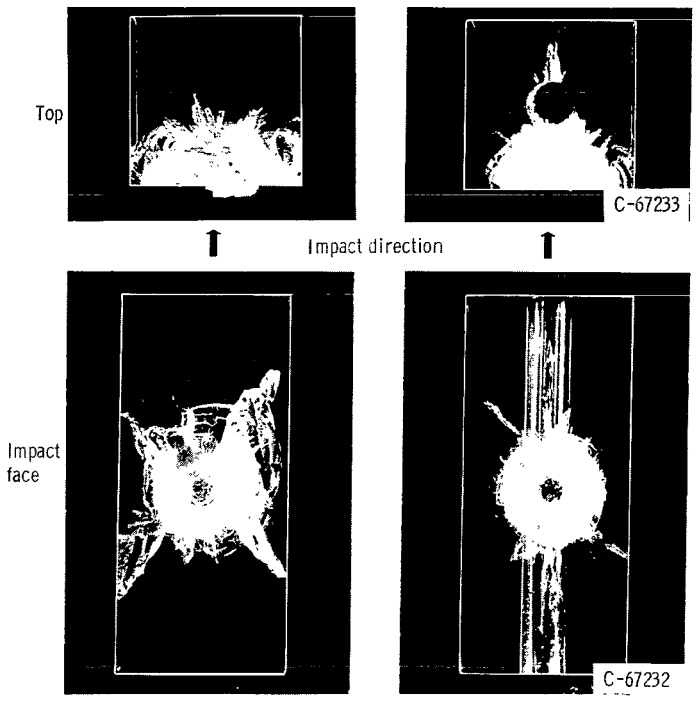

(a) Solid square.

(b) Square with 1/2-inch diameter hole.

Figure 12. - Damage to square prisms (1.77-in. sides, 4-in. length) resulting from impact by 7/32-inch-diameter aluminum spheres at nominal velocity of 6400 feet per second.

cylindrical hole. The square prisms had a volume equal to the volume of the circular cylinders discussed earlier. For the solid square prism, the results shown in figure 12 indicate that the total damage is restricted to the vicinity of the impact point. The damage due to radial fracture and spalling in the area surrounding the impact point is considerably more severe than that obtained with impact into the same volume solid cylinder (fig. 10). The reflected waves produced by the side walls in the square were directed inward toward the centerline of the prism and produced tension fractures and spalling in the crater region, while the reflected waves from the boundaries of the circular cylinder moved downward and away from the crater and produced tensile fractures opposite the crater as described previously.

The results of an impact into a square prism with a hole (fig. 12) indicate longitudinal fractures at the inner surface of the hole, and also slightly less radial fracture and spalling in the vicinity of the impact than in the solid square prism. The axial fracture in the rear portion of the prism is similar to those encountered on cylindrical specimens and is presumed to be caused by the interaction of the reflected wave from the side walls of the specimen. The radial cracks are caused by the expanding dilational wave, as discussed in the section Damage Phenomena.

Specimen size and presence of a hole. - As indicated previously, the amount and type of damage sustained by a brittle target is dependent on the size of the target. To be more specific, the distance of the free boundary from the impact point is a dominant variable. This is manifested in variations in specimen frontal area, specimen thickness, the wall bounding an internal hole, and the size and location of internal holes.

The effects of proximity of boundaries for targets of the same cross sectional area were described previously when the 1.77-inch-square prism (fig. 12) and the 2-inch-diameter cylinder (fig. 10) were compared. The close proximity of the sides in the square prism produced strongly reflected tension waves which caused the large amount

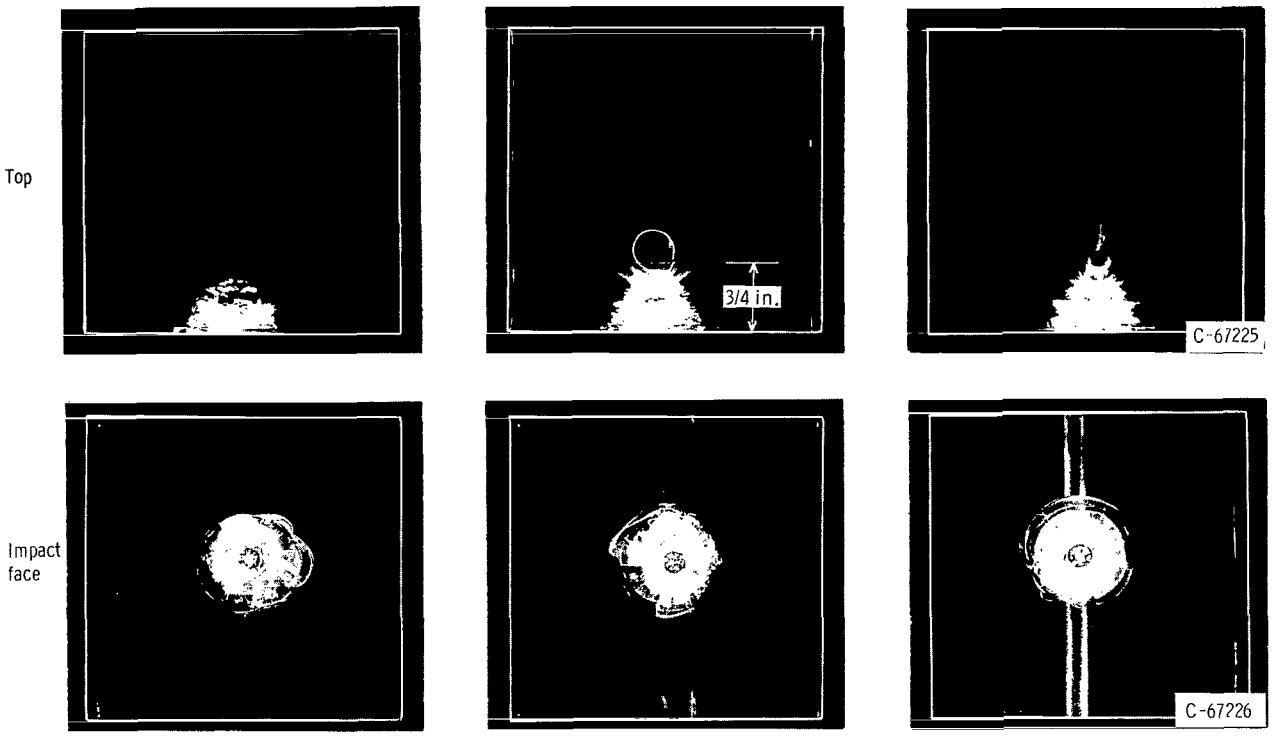

(a) Solid cube.

(b) Cube with 1/2-inch-diameter hole 3/4 inch from impact face.

(c) Cube with 1/4-inch-diameter hole 3/4 inch from impact face

Figure 13. - Results of impact into 4-inch Lucite cubes by 7/32-inch-diameter aluminum spheres at nominal velocity of 6400 feet per second.

of secondary fracture and spalling shown in figure 12. When the sides are located farther from the impact point, the pressure wave is reduced in intensity on reaching the wall with a consequent reduction in intensity in the tension waves and a reduction in spalling and cracking damage. This reduction of damage can also be observed by noting the results of impact into the face of the solid 4-inch cube shown in figure 13. This specimen had a sufficiently large frontal area (separation of side walls) and depth, so that the damage sustained was essentially due to the initial pressure pulse from the impact.

If the same frontal area is maintained but the specimen is made thinner, but not thin enough to permit complete penetration by the projectile, the reflected waves from the rear boundary of the specimen influence the extent of damage in the vicinity of the crater. Spall damage also occurs at the rear boundaries, as shown in the photograph of the results of impact into a 4- by 4- by 1-inch free-standing specimen (fig. 6(a)).

The inclusion of a void or hole close to the impact point reduces the effective specimen thickness. Stress waves caused by impact are reflected from such surfaces, and the reflected tensile waves are directed toward the crater area and result in additional damage. Figure 13 illustrates two such cases and depicts the results of impacting 4-inch Lucite cubes having 1/2- and 1/4-inch-diameter drilled holes. The wall thickness be-

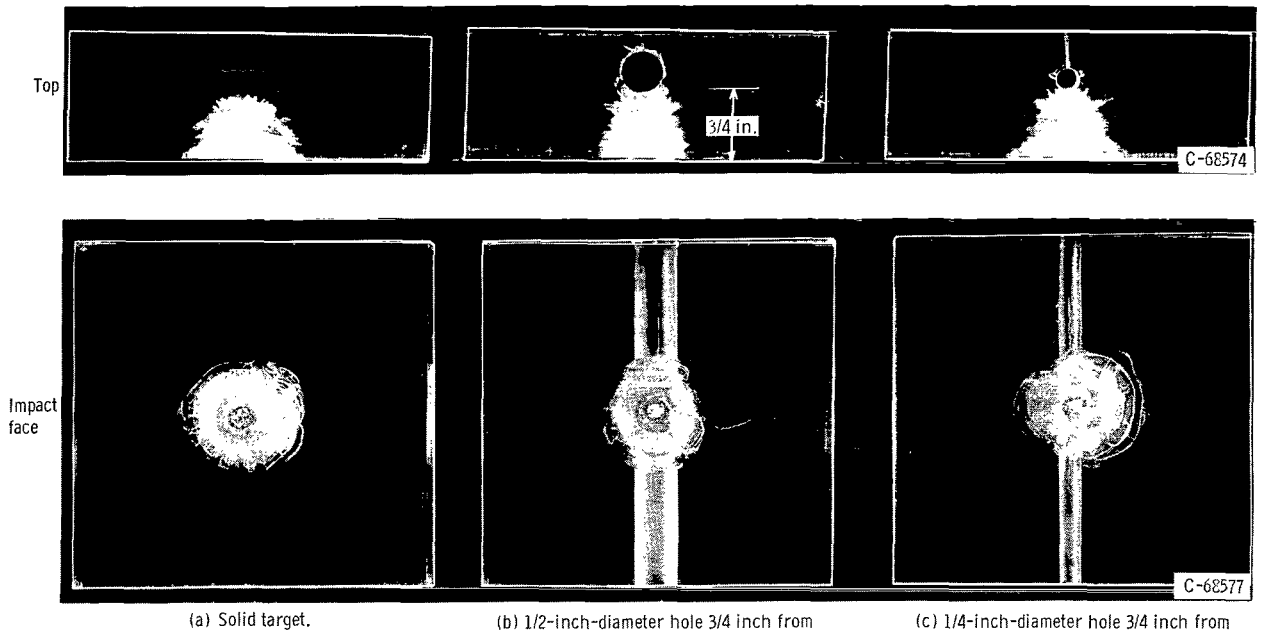

(a) Solid target.

(b) 1/2-inch-diameter hole 3/4 inch from impact face.

(c) 1/4-inch-diameter hole 3/4 inch from impact face.

Figure 14. - Effect of presence and size of internal hole in $1\frac{1}{2}$-inch-thick Lucite targets. Projectiles, 7/32-inch diameter aluminum spheres; nominal velocity, 6400 feet per second.

tween the edge of the hole and the front face of the specimen was maintained constant at 3/4 inch, and the impact was made directly over the point of minimum wall thickness. Both impacts resulted in additional secondary damage in the crater area compared to the solid cube shown in the same figure.

The damage is further aggravated as the overall target thickness is reduced. Figure 14 shows the results of impacts into 4- by 4- by $1\frac{1}{2}$-inch Lucite targets having 1/2- and 1/4-inch-diameter holes drilled through the inside and a 3/4-inch wall thickness. The reduction in target thickness to $1\frac{1}{2}$ inches resulted in fractures on the rear side of each of the drilled specimens, whereas the 4-inch cubes shown in figure 13 had fractures on the rear side of the 1/4-inch-diameter hole only (fig. 13(c)). It is conjectured that the reduction in wall thickness on the rear portion of the $1\frac{1}{2}$ inch-thick targets reduced the ability of the target to resist the deformation and resulted in a fracture. The 1/4-inch-diameter hole drilled into the 4-inch cube provided somewhat the same effect in that the stress-wave components reflected from the boundary of the hole were supported by an insufficient amount of material on the rear side of the hole. The fracture shown in figure 13 is the end result. All drilled specimens exhibited a longitudinal fracture on the front or impact side of the hole and increased damage in the crater area. The reasons for such fractures have been discussed previously.

The impact damage in the solid $1\frac{1}{2}$-inch-thick target (fig. 14(a)) was not greater than in the solid 4-inch cube (fig. 13(a)). A $1\frac{1}{2}$-inch thickness therefore functions as a semi-infinite thickness for the impact conditions used herein.

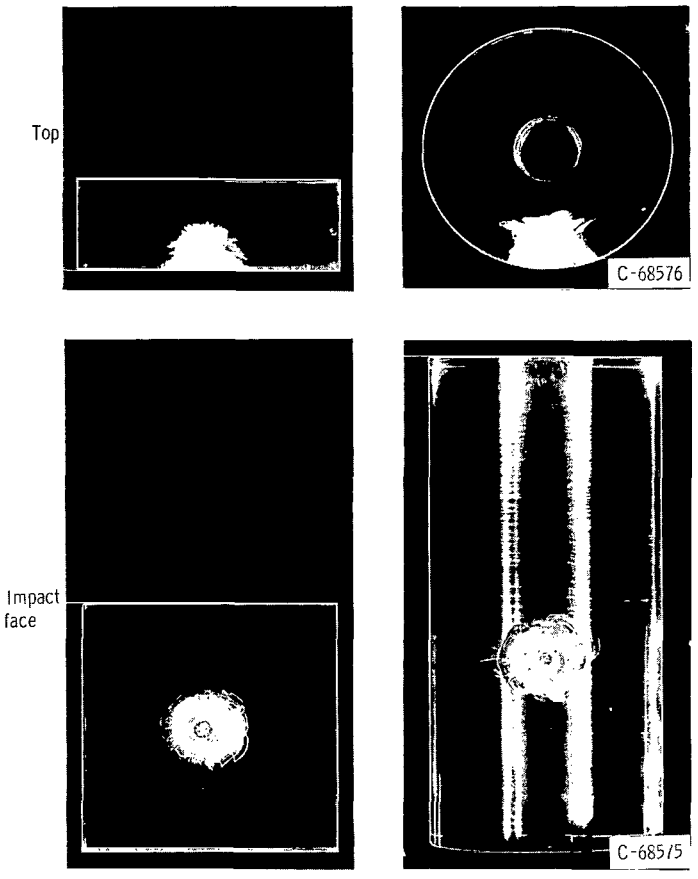

(a) Flat target (infinite radius).

(b) Cylindrical target with 1.85-inch surface radius.

Figure 15. - Results of impact into Lucite targets having constant wall thickness of $1\frac{1}{2}$ inches and various outer surface radii. No rear surface spalling; projectiles, 7/32-inch-diameter aluminum spheres; nominal velocity, 6400 feet per second.

Surface curvature. - The radius of curvature of the target boundaries will influence the initiation and reflection of the impact-induced stress waves and the resulting damage pattern. A series of experiments was performed to investigate the effect of variations in the inner and outer target radius of curvature on the primary and secondary impact damage. A secondary purpose of this phase of the study was to obtain an assessment of the variation in target proportions as a means of damage reduction.

The first experiment compared flat and cylindrical specimens of semi-infinite thickness (wall thickness, $1\frac{1}{2}$ in.). Essentially the same damage pattern was observed for a 4- by 4- by $1\frac{1}{2}$-inch-thick target and a cylindrical target 3.7 inches in diameter having a $1\frac{1}{2}$-inch-thick wall (fig. 15). No secondary spalling on the rear portion of either of the targets was observed. The slight difference in the appearance of the primary fracture in the cylinder was attributed to a striation present in the material as received.

The next experiment involved impacts into finite-thickness cylinders of Lucite and studied the effects of a variable radius of curvature on the resulting secondary damage. The results are shown in figure 16 and illustrate the effectiveness of the cylindrical shape in suppressing secondary spall from the rear surface of the target. All the targets shown had a constant wall thickness of 3/4 inch. The primary and secondary spall impact fractures had the same appearance in the 3/4-inch-thick flat plate and the largest cylinder (fig. 16(b)). When the target surface radius was reduced to $1\frac{1}{8}$ inches, the secondary rear spall was eliminated. Targets having surface radii of 1 inch and 7/8 inch were also tested with the same results; however, increasing amounts of radial and rear fracturing were observed as the outer radius decreased.

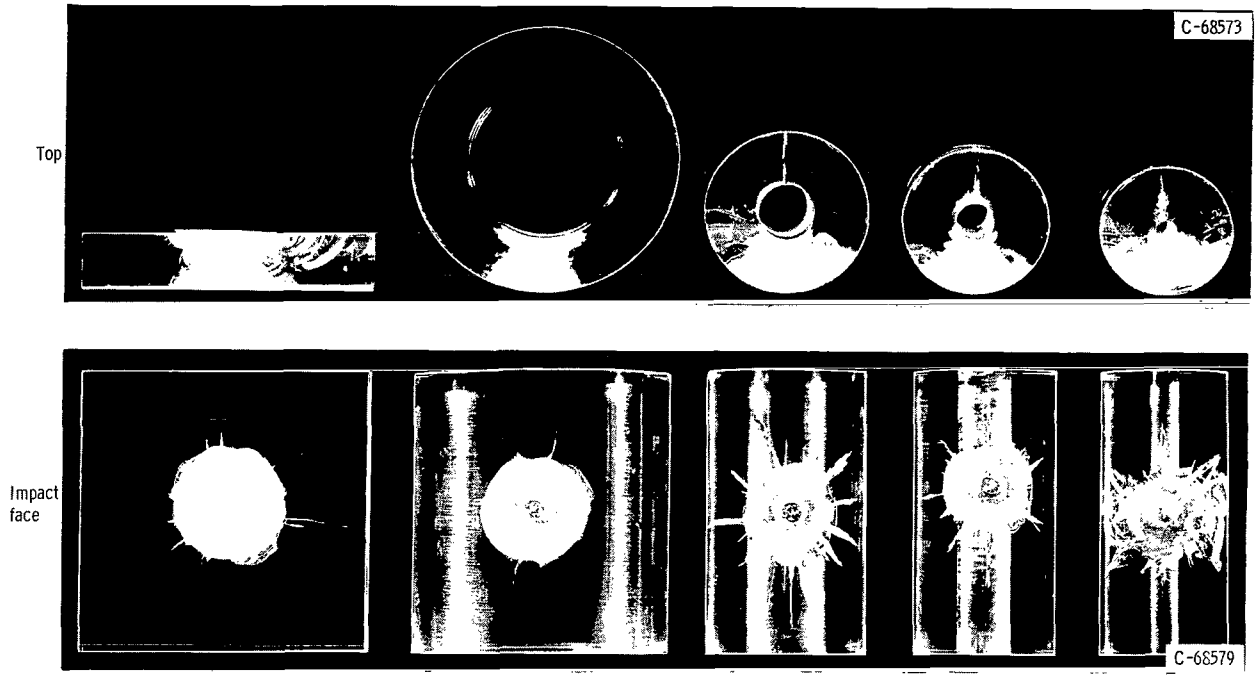

(a) Flat target (infinite surface radius). (b) Cylindrical target with 1.85-inch surface radius. (c) Cylindrical target with 1 1/8-inch surface radius. (d) Cylindrical target with 1-inch surface radius. (e) Cylindrical target with 7/8-inch surface radius.

Figure 16. - Results of impact into Lucite targets having constant wall thickness of 3/4 inch and various outer surface radii. Spalling on rear surface of impacted side; projectiles, 7/32-inch-diameter aluminum spheres; nominal velocity, 6400 feet per second.

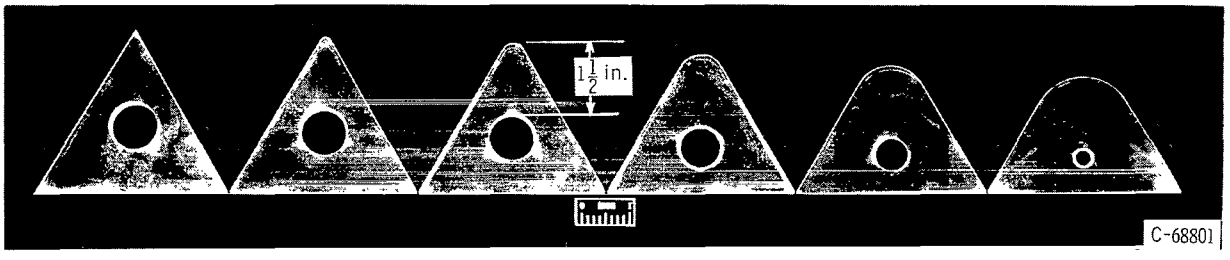

(a) Before impact.

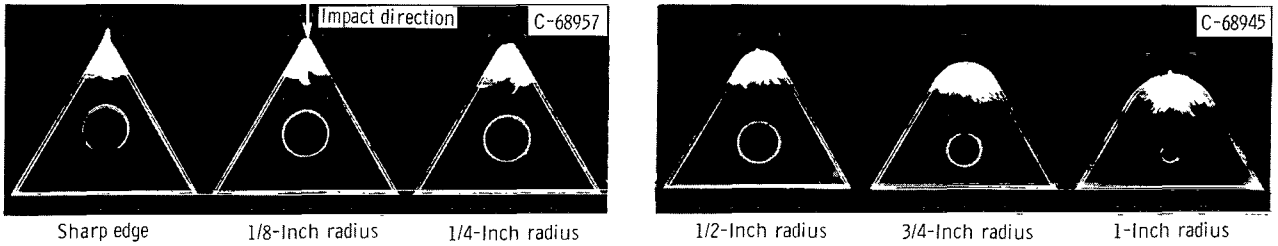

Sharp edge 1/8-Inch radius 1/4-Inch radius 1/2-Inch radius 3/4-Inch radius 1-Inch radius

(b) After impact.

Figure 17. - Results of impact into constant-mass triangular prisms having various surface radii at impacted edge. Wall thickness, $1\frac{1}{2}$ inches; Projectiles, 7/32-inch-diameter aluminum spheres; nominal velocity, 6400 feet per second.

The secondary rear surface spall was produced in the flat target (fig. 16(a)) and the largest cylinder (fig. 16(b)) because the reflection of the stress wave on the rear surface occurred with peak intensity over a finite area. The material was subsequently dislodged as a secondary spall. As the target surface radius was decreased, the zone of peak intensity of the reflected wave was reduced to a narrow band or line along the axis of the bore, and this resulted in a longitudinal fracture. Longitudinal fractures appeared on the rear side of the cylindrical targets having surface radii of $1\frac{1}{8}$, 1, and 7/8 inch.

The primary crater depths were measured on this series of targets in an effort to obtain a correlation with tube curvature; however, the measurements did not indicate a significant trend.

In general, the amount of visually observed damage tended to increase as the target surface radius decreased. This was due to the combined effects of increased confinement of the reflected stress waves by the outer boundary, the reduction of effective target mass, and the presence and the diameter of the central hole.

To better isolate the effect of a variation in the external radius on target damage, a series of impacts was made into constant-mass targets with varying radius of curvature at the impact point. The targets used, shown in figure 17, were triangular prisms with an axial hole. The distance from the curved impact surface to the nearest edge of the holes was held constant at $1\frac{1}{2}$ inches, and the diameter of the hole was varied to maintain constant target mass. The results of impact, shown in figure 17, did not indicate a significant change in observable damage with a change in external radius. Also, the measured crater depths did not change with a variation in the external radius.

Prior experiments of impacts into a 4-inch cube without a hole (fig. 13(a)), a 4-inch cube with a 1/2-inch-diameter hole (fig. 13(b)), and a 4-inch cube with a 1/4-inch-diameter hole (fig. 13(c), p. 25) indicated that the presence and size of a hole can result in increased secondary damage. It can be seen in figure 13 that the presence of the hole increases the damage in the impact region because of the reflected wave from the inner hole boundary under the impact point. Also, the smaller size hole produced secondary damage that started on the rear side of the hole and progressed toward the rear of the specimen. It was felt that this fracture was induced by the reflected components of the incident wave. This observation suggests that small-diameter holes or voids in close proximity to the impact point will aid the propagation of secondary fractures.

Abrupt changes in cross section. - A problem more specifically related to space radiators is the attachment of thin radiating fins to the more massive meteoroid protective armor surrounding the fluid carrying tube. It was felt that the abrupt change in cross section between fin and armor could produce an effect similar to that of targets having small-diameter holes. A complete investigation of the wide range of geometries and variables is beyond the scope of this report. However, it was felt that a valuable

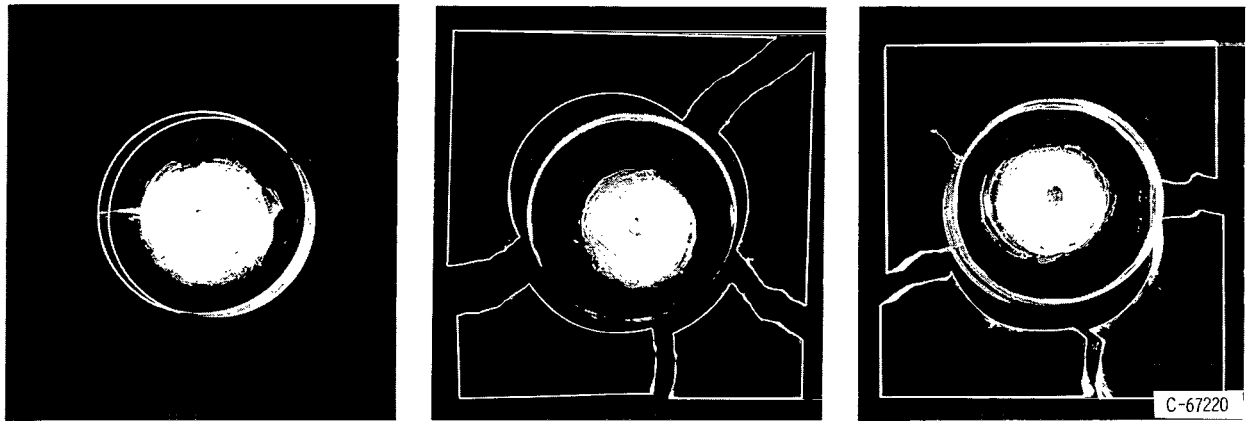

No fin | 1/ 8-inch-thick fin | 1/ 4-inch-thick fin

(a) No fillet between central hub and fin.

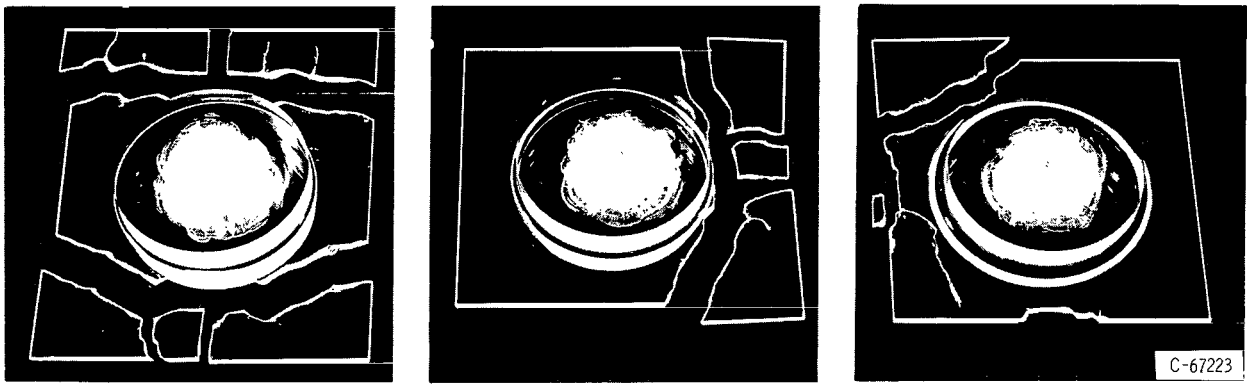

1/16-inch radius | 1/8-inch radius | 1/4-inch radius

(b) Fillet radius variation between central hub and 1/8-inch-thick fin.

Figure 18. - Effect of abrupt changes in cross section on 1-inch-thick Lucite targets. Projectiles, 7/32-inch-diameter aluminum spheres; nominal velocity, 6400 feet per second.

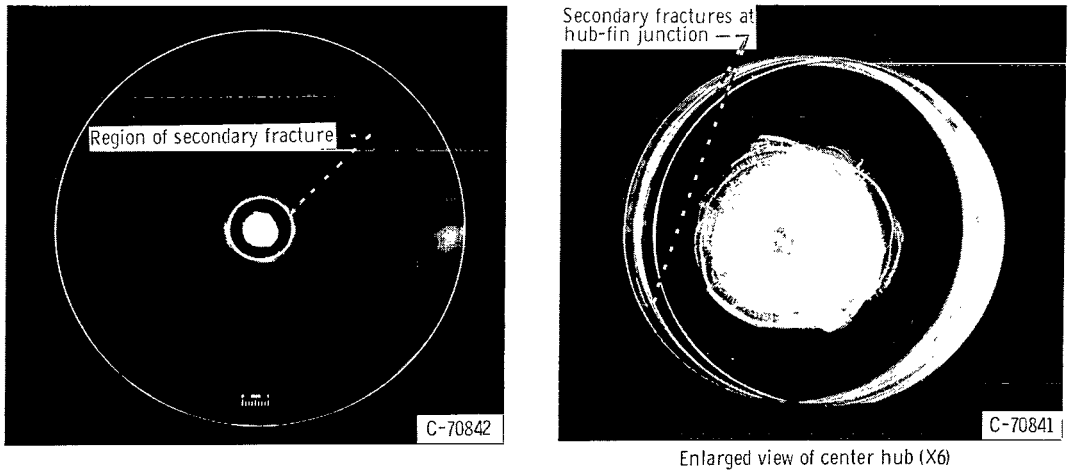

Enlarged view of center hub (X6)

Figure 19. - Effect of abrupt changes in cross section on 1-inch-thick circular Lucite targets having 1/8-inch-thick fin and 16-inch outside diameter. Projectile, 7/32-inch diameter aluminum spheres; nominal velocity, 6400 feet per second.

insight could be gained by testing the behavior of abrupt changes in cross section under impact conditions in simple Lucite targets.

A series of models was designed, each machined in one piece from 4- by 4- by 1-inch cast Lucite blocks. All specimens had a $2\frac{1}{2}$-inch-diameter hub 1 inch thick surrounded by a thin square central fin sheet. The variations machined in the specimens were the fillet radius at the hub-fin joint and the fin thickness.

The effect of no fillet radius at the hub-fin junction on fins of 1/8 and 1/4 inch thickness is illustrated in figure 18(a). In both cases, the fins were completely severed from the hub by the reflected tensile waves interacting with the sharp corners. The change in fin thickness had little effect on this phenomenon.

Figure 18(b) illustrates the reduction in fin damage possible by increasing the hub-fin fillet radius. The specimens all have a fin thickness of 1/8 inch and fillet radii of 1/16, 1/8, and 1/4 inch; however, it was felt that the specimen size contributed to the damage pattern observed. To study this effect better, a second series of models was prepared from a single piece of Lucite in the form of disks having the same hub diameters, fin thicknesses, and fillet radii as the square targets tested previously, but having a circular fin shape. The overall fin diameter was varied between 8 and 16 inches to reduce the effects of specimen size on the secondary fractures. The results contrasted those obtained previously in that only the specimens having no fillet radii were fractured at the hub-fin junction (fig. 19). The incorporation of a 1/16-inch radius was sufficient to suppress the fracture at the change in cross section. In actual practice, when a brittle material such as beryllium is employed as radiator fins, the brittle fractures just discussed may become a reality and may become of concern to the radiator designer.

Reduction of Secondary Damage

The experiments thus far have demonstrated that secondary damage can occur in the form of internal fractures and rear surface spalls and that the origin of the secondary damage is the reflected component of the initial stress wave. One method of reducing this type of damage in joined members employed the use of large fillet radii for the corners of joined members. Increasing the size and increasing the radius of hollow cylindrical members will also be beneficial for secondary damage reduction. The previously discussed results of thick nonperforated Lucite sheets indicated that placing other materials in contact with the free surfaces was beneficial in reducing secondary damage. However, placing other materials in contact with the free surface of Lucite sheets sufficiently thin to be completely penetrated by the projectile produced increased secondary damage compared to that in an unbacked target of the same thickness. The only means available of reducing secondary damage in targets that will be completely penetrated is

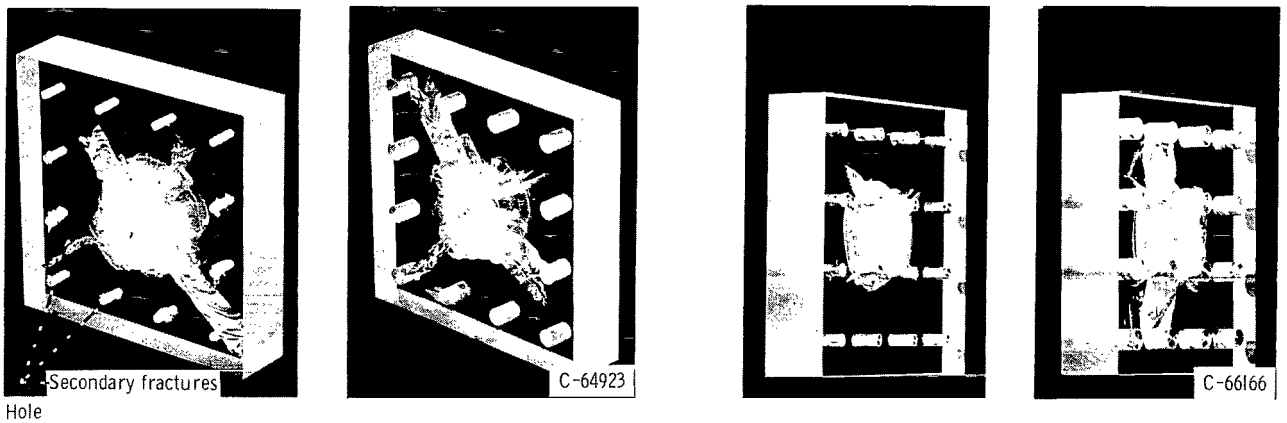

Figure 20. - Results of impact into 4- by 4- by 1-inch-thick Lucite specimens containing internal holes. Projectiles, 7/32-inch-diameter aluminum spheres; nominal velocity, 6400 feet per second.

to reduce the wall thickness. In view of the variation in impact damage in the composite targets previously tested, the concept of multiple-layered media for nonperforated targets was extended, and the results of this further investigation are discussed in the following section.

Treatment of internal boundaries. - The effect of high acoustic impedance inserts inside the target volume was studied for both flat and cylindrical specimens. The results of impact into 4- by 4- by 1-inch cast Lucite blocks with a series of holes drilled through the 1-inch thickness to illustrate the effect of voids are shown in figure 20. Holes of 1/4-inch diameter and 1/8-inch diameter were employed. The long radial fractures shown in figure 20(a) are more severe than those observed for the solid specimen shown in figure 6(a). The presence of the hole causes reflections of the incident pressure wave close to the point of impact, and the resulting reflected tensile wave causes fractures. More damage and radial fracturing was observed in the target having the 1/8-inch-diameter holes than in the target with the 1/4-inch-diameter holes. This observation further indicates that hole size has an effect on observed secondary damage.

Figure 15(b) (p. 27) illustrates the effect of placing a material of higher acoustic impedance than the target material inside the voids. Soft aluminum pins were machined to fit snugly in the voids and proved to be effective in reducing the secondary damage by suppressing the fractures emanating from the 1/8- and 1/4-inch-diameter holes. The reflections at the aluminum-Lucite interface became compressive instead of tensile and consequently produced smaller relative damage. The aluminum pin in the 1/8-inch-diameter hole effectively nullified the stress concentration of the hole itself. However, the resulting damage continued to be more severe than that observed in a solid target without holes (fig. 6(a), p. 16) for both configurations tested.

A second series of tests used concentric cylinders of Lucite, steel, and aluminum

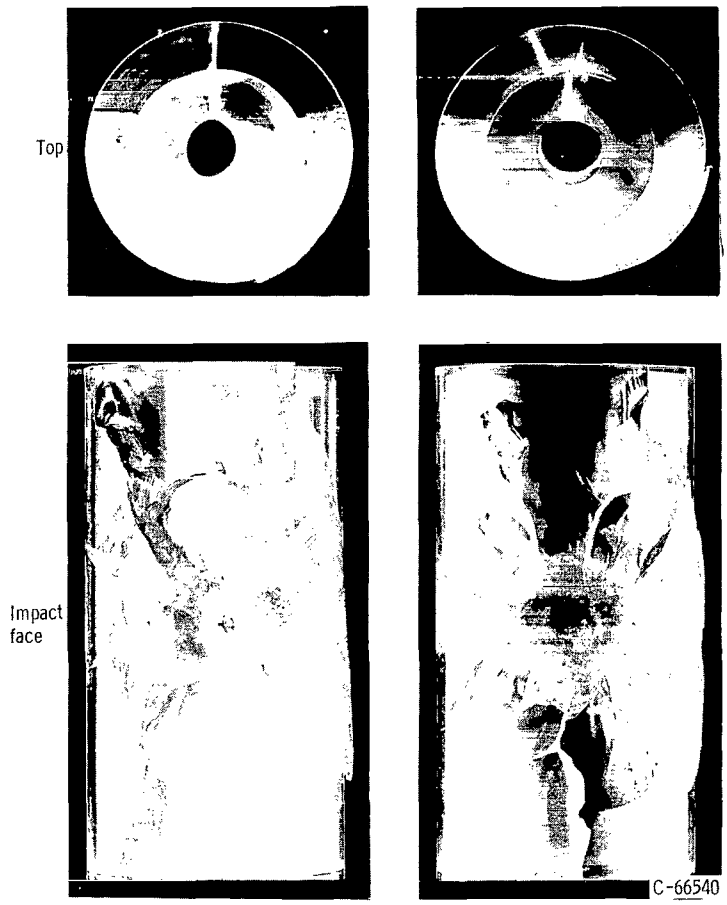

(a) Lucite to Lucite interface.

(b) 1/200-Inch aluminum between interfaces.

Figure 21. - Results of impact into nested concentric cylinders having 3/8-inch wall thickness. Assembled dimensions, 2-inch outside diameter, 1/2-inch-diameter bore; projectiles, 7/32-inch-diameter aluminum spheres; nominal velocity, 6400 feet per second.

in various combinations as a possible means of reducing secondary damage. Bimetallic composite-walled tubes are frequently encountered in space vehicles since the interior and exterior environments can differ widely (ref. 2). The first series of tests consisted of closely fitting nested concentric Lucite cylindrical tubes having a maximum external diameter of 2 inches and a central hole of 1/2-inch diameter. The outer Lucite tube wall was approximately 3/8 inch thick, which was sufficiently thin to be completely penetrated by the projectile. The mating surfaces of the two cylinders were machined to fit and assembled without cement. Figure 21 shows the results of impact into concentric Lucite cylinder targets. The observed secondary damage on the outer surface of the cylinders is much more severe than that in a single tubular Lucite cylinder (fig. 10). The insertion of 0.005-inch-thick aluminum foil at the interface between the inner and outer cylinders was not effective in reducing the observed damage (fig. 21(b)). Since the outer

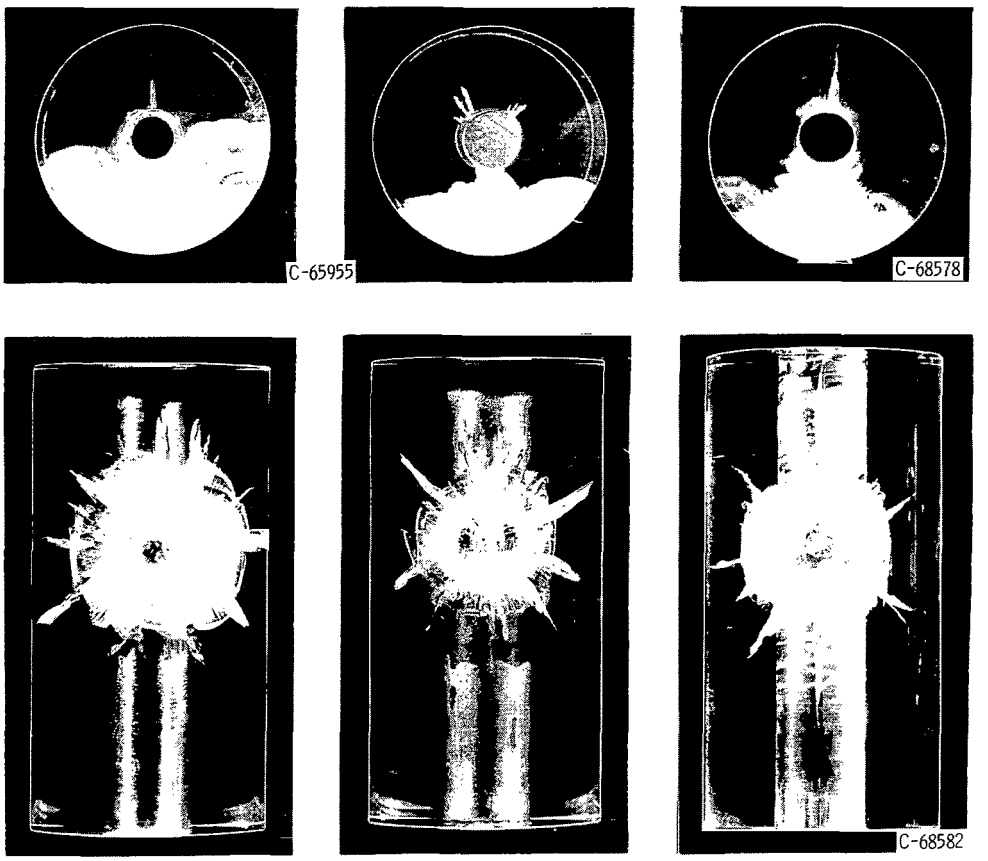

(a) Tubular insert with 1/2-inch outside diameter and 0.060-inch-thick wall.

(b) Solid insert with 1/2-inch outside diameter.

(c) Aluminum projectile, hollow cylinder. 1/2 in. diam. bore.

Figure 22. - Results of impact into Lucite cylinders having 2-inch outside diameter and 1/2-inch-diameter bore containing stainless steel inserts. Projectiles, 7/32-inch-diameter aluminum spheres; nominal velocity, 6400 feet per second.

cylinder was completely penetrated by the projectile, the inner tubular member and foil interface participated in the primary fracturing process and induced additional damage in the outer member. A discussion of this phenomenon was presented in an earlier section (Thin Lucite Sheet) and thus will not be repeated here. The indications here tend to cite the need to locate an interface as far as possible from the point of impact to reduce damage to a minimum.

Additional test specimens were fabricated for the purpose of determining whether a centrally located high-acoustic-impedance insert is effective in reducing secondary damage in the crater area of a tubular specimen. These specimens consisted of a 2-inch-diameter cast Lucite cylinder 4 inches long with a 1/2-inch-diameter hole bored along the central axis. These specimens were fitted with stainless-steel inserts (both tubular and solid), which were cemented into the 1/2-inch-diameter hole with ethylene dichloride cement. The results shown in figure 22 indicate that the use of inserts had a minor

effect in reducing the overall target damage.

Treatment of external boundaries. - It was indicated earlier that, to reduce the severity of the secondary damage fracture at the rear half of cylindrical bodies, the external boundaries of the cylinder can be surrounded by a material of high acoustic impedance. The use of such a sleeve produces a reflected wave of the same sign as the incident wave and depending on the sleeve thickness reduces the intensity of these waves in the target. Cylinders having a 2-inch outside diameter, a length of 4 inches, and a central 1/2-inch-diameter hole bored along the longitudinal axis were tightly wrapped with aluminum sheet or foil. A 1/2-inch-wide strip of the sleeve material was removed for the full length of the specimen to permit impact directly into the Lucite. The results shown in figure 23 illustrate the effect of increasing sleeve thickness. A 0.005-inch foil sleeve (fig. 23(a)) was relatively ineffective in reducing the secondary damage at the rear of the specimen; however, thicknesses of 1/16 inch (fig. 23(b)) and 1/8 inch (fig. 23(c)) did serve with increasing effect to reduce the rear secondary fracture damage. The damage in the front portion of the tubes exhibited the opposite trend and increased as sleeve thickness increased.

It was felt that wave interactions with the edges of the gap in the sleeve had contributed to the damage obtained in these targets. Another specimen was fashioned which embodied a full circumferential sleeve of aluminum 1/8 inch thick machined to fit the Lucite cylinder. The sleeve had a 1/2-inch-diameter hole bored through one wall, through which the impact was made into the Lucite. The results shown in figure 23(d) indicate that the fracture in the rear of the specimen was eliminated and the damage in the front portion of the cylinder was reduced below the level encountered in specimens having a wrapped sleeve with a longitudinal gap (figs. 23(a), (b), and (c)). The results from this last series of experiments confirm that internal fractures in the rear half of cylindrical specimens can be suppressed by the application of a high-acoustic-impedance material to the outer boundary if sleeves of substantial thicknesses are employed.

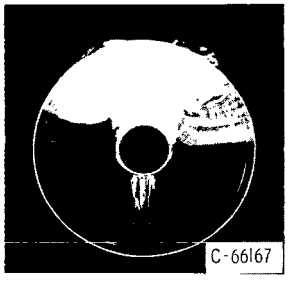

(a) Partial sleeve of .005-inch thick aluminum; 1/2-inch gap.

(b) Partial sleeve of 1/16-inch-thick aluminum; 1/2-inch gap.

(c) Partial sleeve of 1/8-inch-thick aluminum; 1/2-inch gap.

(d) Full sleeve of 1/8-inch-thick aluminum; 1/2-inch-diameter hole at impact point.

Figure 23. - Results of impact into Lucite cylinders having 2-inch-outside diameter and 1/2-inch-diameter bore with external aluminum sleeves of varying thickness. Projectiles, 7/32-inch-diameter aluminum spheres; nominal velocity, 6400 feet per second.

CONCLUSIONS

The following conclusions were reached in an investigation of damage to glass and Lucite by impact with high-velocity projectiles:

1. Fractures in brittle materials caused by impacting high-velocity projectiles can be divided into two broad classes:
   a. Primary fractures caused by the initial impact (e.g., crater and radial dilatation fractures)
   b. Secondary fractures caused by the interaction between the reflected stress-wave components from a free surface or interface (e.g., rear surface spall and internal fractures)
2. The primary fractures occurring for a particular target geometrical shape, brittle material, and set of impact conditions are unique. Consequently, the location of these fractures cannot be altered, and their severity cannot be reduced.
3. The secondary fractures in the brittle target are dependent upon the target shape, size (i.e., proximity of the free edges), and adjacent materials in contact with the free edges. The location and the severity of these fractures are both controllable.
4. Voids or holes inside the target act as free surfaces, reduce the effective size of the target, and consequently produce increased secondary damage. Experimental evidence points toward the fact that small-diameter holes act as stress raisers and propagate or initiate secondary fractures.
5. Abrupt changes in cross sections with sharp corners act as stress raisers and induce secondary damage in the target. Incorporating even small corner radii is effective in reducing the severity of the secondary damage.
6. The most effective method of controlling the severity of the secondary damage for a given geometrical shape that is not completely penetrated by a projectile is by placing a material with a higher acoustic impedance than the target material in the voids within the target or on the free surfaces of the target. Flat plate targets having filled internal voids, however, continue to exhibit a greater degree of secondary damage than will a solid target of the same material. Application of a higher acoustic impedance backing or layers on the active external surfaces of the target is effective in reducing the secondary damage effects in the target.
7. For targets sufficiently thin to be completely penetrated by a projectile, the total damage to the target decreased as the target thickness was reduced. Placing materials with higher acoustic impedance adjacent to the target can increase damage.

8. The impact behavior of a specific specimen shape or cross section should be determined by testing or analyzing the cross section itself since secondry impact damage is strongly dependent on target size and shape.

Lewis Research Center,
National Aeronautics and Space Administration,
Cleveland, Ohio, January 5, 1965.

REFERENCES

1. Krebs, Richard P., Winch, David M., and Lieblein, Seymour: Analysis of a Megawatt Level Direct Condenser-Radiator. Prog. in Astronautics and Aeronautics. Vol. 11 - Power Systems for Space Flight, Academic Press, Inc., 1963, pp. 475-504.

2. Diedrich, James H., and Lieblein, Seymour: Materials Problems Associated with the Design of Radiators for Space Powerplants. Prog. in Astronautics and Aeronautics. Vol. 11 - Power Systems for Space Flight, Academic Press, Inc., 1963, pp. 627-653.

3. Loeffler, I. J., Lieblein, Seymour, and Clough, Nestor: Meteoroid Protection for Space Radiators. Prog. in Astronautics and Aeronautics. Vol. 11 - Power Systems for Space Flight, Academic Press, Inc., 1963, pp. 535-549.

4. Gehring, J. W., Christman, D. R., and McMillan, A. R.: Hypervelocity Impact Studies Concerning the Meteoroid Hazard to Aerospace Materials and Structures. CP-8, AIAA Fifth Annual Structures and Materials Conf., Palm Springs (Calif.) Apr. 1-3, 1964.

5. Diedrich, J. H., Loeffler, I. J., and Stepka, F. S.: Brittle Behaviour of Beryllium, Graphite, and Lucite Under Hypervelocity Impact. NASA TM X-52062, 1964.

6. Reinhart, John S.: Impact Craters in Rock. TR-60-39, Vol. III, Fourth Symposium on Hypervelocity Impact, Air Proving Ground Center, Sept. 1960.

7. Kinslow, Ray: Properties of Spherical Stress Waves Produced by Hypervelocity Impact. AEDC-TDR-63-197, Aro, Inc., Oct. 1963.

8. Reinhart, John S.: On Fractures Caused by Explosives and Impacts. Colorado School of Mines Quarterly, vol. 55, no. 4, Oct. 1960.

9. Pearson, John: The Explosive Working of Metals. NAVORD Rep. 7033, Naval Ord. Test Station, Feb. 4, 1960, pp. 14-15.

10. Eshbach, O. W.: Handbook of Engineering Fundamentals. John Wiley & Sons, Inc., 1936, sec. 1-121.

11. Anon.: Plexiglas-Design and Fabrication Data. Bull. 229g, Rohm and Haas Co., 1961, p. 2.

12. Forsythe, William Elmer: Smithsonian Physical Tables. Ninth ed., Smithsonian Inst., Wash. D.C., 1954.

13. Stepka, Francis S., and Morse, C. Robert: Preliminary Investigation of Catastrophic Fracture of Liquid-Filled Tanks Impacted by High-Velocity Particles. NASA TN D-1537, 1963.

14. Malik, D.: An Empirical Study on Residual Velocity Data for Steel Fragments Impacting on Four Materials. Proc. Third Symposium on Hypervelocity Impact, Vol. II, Armour Res. Foundation, Chicago (Ill.), Oct. 7-9, 1958.

"The aeronautical and space activities of the United States shall be conducted so as to contribute . . . to the expansion of human knowledge of phenomena in the atmosphere and space. The Administration shall provide for the widest practicable and appropriate dissemination of information concerning its activities and the results thereof."

—NATIONAL AERONAUTICS AND SPACE ACT OF 1958

NASA SCIENTIFIC AND TECHNICAL PUBLICATIONS

TECHNICAL REPORTS: Scientific and technical information considered important, complete, and a lasting contribution to existing knowledge.

TECHNICAL NOTES: Information less broad in scope but nevertheless of importance as a contribution to existing knowledge.

TECHNICAL MEMORANDUMS: Information receiving limited distribution because of preliminary data, security classification, or other reasons.

CONTRACTOR REPORTS: Technical information generated in connection with a NASA contract or grant and released under NASA auspices.

TECHNICAL TRANSLATIONS: Information published in a foreign language considered to merit NASA distribution in English.

TECHNICAL REPRINTS: Information derived from NASA activities and initially published in the form of journal articles.

SPECIAL PUBLICATIONS: Information derived from or of value to NASA activities but not necessarily reporting the results of individual NASA-programmed scientific efforts. Publications include conference proceedings, monographs, data compilations, handbooks, sourcebooks, and special bibliographies.

Details on the availability of these publications may be obtained from:

SCIENTIFIC AND TECHNICAL INFORMATION DIVISION

NATIONAL AERONAUTICS AND SPACE ADMINISTRATION

Washington, D.C. 20546